NOTICE

The quality of this microform is heavily dependent upon the quality of the original thesis submitted for microfilming. Every effort has been made to ensure the highest quality of reproduction possible.

If pages are missing, contact the university which granted the degree.

Some pages may have indistinct print especially if the original pages were typed with a poor typewriter ribbon or if the university sent us an inferior photocopy.

Previously copyrighted materials (journal articles, published tests, etc.) are not filmed.

Reproduction in full or in part of this microform is governed by the Canadian Copyright Act, R.S.C. 1970, c. C-30.

AVIS

La qualité de cette microforme dépend grandement de la qualité de la thèse soumise au microfilmage. Nous avons tout fait pour assurer une qualité supérieure de reproduction.

S'il manque des pages, veuillez communiquer avec l'université qui a conféré le grade.

La qualité d'impression de certaines pages peut laisser à désirer, surtout si les pages originales ont été dactylographiées à l'aide d'un ruban usé ou si l'université nous a fait parvenir une photocopie de qualité inférieure.

Les documents qui font déjà l'objet d'un droit d'auteur (articles de revue, tests publiés, etc.) ne sont pas microfilmés.

La reproduction, même partielle, de cette microforme est soumise à la Loi canadienne sur le droit d'auteur, SRC 1970, c. C-30.

Canada

Bandwidth-Efficient Constant-Envelope Differential PSK Signals

Slimane Ben Slimane

A Thesis

in

The Department

of

Electrical and Computer Engineering

Presented in Partial Fulfillment of the Requirements
for the Degree of Master of Engineering at
Concordia University
Montréal, Québec, Canada

September, 1987

ISBN 0-315-44241-7

ABSTRACT

Bandwidth-Efficient Constant-Envelope Differential PSK Signals

Slimane Ben Slimane

A differential phase shift keying (DPSK) modulation/demodulation scheme with compact bandwidth, constant envelope, simple and fast demodulation is introduced. These properties make the proposed DPSK modulation/demodulation scheme attractive in Time Division Multiple Access (TDMA) applications using nonlinear amplification.

The power spectral density function of these signals is derived. Illustrative results indicates that while maintaining the envelope constant these signals have compact spectra with fast side-lobe roll-off.

The error probability performance of DPSK signals in an additive white Gaussian noise (AWGN) environment is derived. The effects of the low-pass filter on the receiver performance when the phase noise is non-additive and non-Gaussian are studied using a numerical technique.

ACKNOWLEDGEMENTS

I would like to express my deep gratitude to my thesis supervisor Dr. Tho Le-Ngoc for his invaluable assistance and constant guidance throughout this research, and for his advice and constructive criticism during the preparation of this thesis.

I would also like to express my appreciation to the University Mission of Tunisia for its financial support.

I am grateful to the support and patience of my family. Last but not least I would like to thank all my friends for their encouragement throughout my studies. like all

Table of Contents

LIST OF PRINCIPAL SYMBOLS

A	Carrier amplitude
a_n	Binary symbol
p(t)	wave shape
K	Integer defining the length of the wave shape
T_b	Bit time interval
f_0	Nyquist frequency, $f_0 = \frac{1}{2T_b}$
f_c	Carrier frequency
$r(t,\alpha)$	Square root raised cosine pulse
$R(f,\alpha)$	Transfer function of the raised cosine pulse
z(t)	PSK transmitted signal
s(t)	Baseband signal (complex envelope)
$R_s(\tau)$	Autocorrelation function of s(t)
S(f)	Fourier transform of $R_s(\tau)$
$b(t,\underline{a}_n) = \exp\left[j\frac{\pi}{2}\sum_{i=-\infty}^{+\infty} a_{n-i}\, p(t+iT_b)\right]$	
$B(f,\underline{a}_n)$	Fourier transform of $b(t,\underline{a}_n)$
$R_{b,n}(t,t') = \overline{b(t,\underline{a}_n)b^*(t',\underline{a}_0)}$	
$S_{b,i}(f)$	Fourier transform of $R_{b,i}(t,t')$

$S_d(f)$	Discrete part of the power spectral density
$S_c(f)$	Continuous part of the power spectral density
$h_i(t) = p(t + iT_b)\prod\left(\frac{t + (K-i)T_b}{T_b}\right)$	
N_c, N_s	Sample values of additive white Gaussian noise
N(t)	Random amplitude function
$f_Y(y)$	Probability density function of the random variable Y
Ψ_i	Phase of the ith received vector
$\Phi_Y(\omega)$	Characteristic function of the random variable Y
$erf(x)$	error function, $erf(x) = \frac{2}{\sqrt{\pi}}\int_0^x e^{-u^2}du$
$Pr(error/\Psi)$	Probability of error given the random variable Ψ
Pe	Average probability of error
$\phi(t), \theta(t)$	Phase functions
d	Time interval that is made vanishingly small
h(t)	Impulse response function of equivalent low-pass filter
c_n	Fourier series component
$\tan^{-1}(x)$	Inverse of tan(x)
$f^*(x)$	Complex conjugate of $f(x)$
$\overline{f(x, a_i)}$	Statistical average
E(X)	Expected value of X
$\bar{X} = E(X)$	

List of Figures

CHAPTER ONE

INTRODUCTION

Modulation is one of the most important operations to transmit information over a communication channel. Its primary objectives are to use the bandwidth and signal-to-noise ratio as efficient as possible while maintaining a good transmission quality for a given amount of information. Pursuing these objectives, many digital modulation techniques have been proposed. The need for power and bandwidth efficient modulation schemes has led to the extensive use of phase-shift keying (PSK) in digital transmission systems and particularly for non-linear channels.

To maximize the power efficiency of a transmitter, its high power amplifier (HPA) is desired to operate in a non-linear or even saturation mode. For multi-carrier transmitters, non-linear power amplifiers can not be used because of the limitation due to the intermodulation distortion. In TDMA (Time Division Multiple Access) systems, since the transmitter contains only one modulated carrier, its power amplifier can operate at saturation without any intermodulation product. However, the non-linear characteristics, namely AM/AM and AM/PM conversions, can cause spectrum spreading and distortion due to cross-talk if the input signal to the power amplifier contains a certain amplitude (envelope) fluctuation. Spectrum spreading implies a regrowth of spectral side-lobes previously filtered [11]. The extra but unnecessary spectral regrowth increases the amount of interference into adjacent channels and, hence, increases the channel spacings or reduces the number of allocated channels in a given frequency band. Signal dis-

tortion introduces a degradation in the system performance. One solution to overcome this problem is to use constant-envelope modulation schemes with high bandwidth efficiency and a good detection performance.

Coherent demodulation techniques provide a good detection performance at the expense of carrier recovery complexity and long acquisition time. In TDMA applications, short acquisition is desired to reduce the TDMA burst preample and hence to increase the TDMA efficiency. This makes differential demodulation techniques more attractive. Differential demodulation schemes are also more robust than the coherent ones in the presence of Doppler and fast multipath fading effects such as in a mobile communication environment [11].

In this thesis, a bandwidth-efficient constant-envelope Differential Phase Shift Keying (DPSK) modulation/demodulation technique is introduced and studied. This modulation/demodulation scheme provides a *constant-envelope* modulated signal which can be used with saturated power amplifiers for high spectral efficiency. The differential demodulation structure is used with a narrow low-pass filter to improve the detection performance. Although the study presented in this thesis is concentrated on the binary DPSK, its results can be applied to multilevel DPSK.

1.1 Thesis outline

After this introductory Chapter, the proposed bandwidth-efficient constant-envelope DPSK modulation/demodulation described in Chapter 2. At first, the needs of constant-envelope modulated signals and rapid demodulation techniques in TDMA applications are reviewed. The conventional DPSK modulation/demodulation scheme is then discussed. The Chapter ends with the

concepts of the introduced bandwidth-efficient, constant-envelope DPSK modulation/demodulation schemes.

In Chapter Three, the spectral properties of bandwidth-efficient constant-envelope differential PSK signals are investigated. The power spectral density (PSD) function of these signals are presented and discussed.

The performance of bandwidth-efficient constant-envelope differential PSK is studied in Chapter Four. The probability density function (pdf) of the non-Gaussian phase between the two successive received vectors, and the average probability of bit error are derived. A numerical method to compute this pdf is introduced.

Chapter Five contains conclusions and suggestions for further studies.

1.3 Research contributions

The major contributions of this research include the analytical studies of the spectral properties and performance of a proposed bandwidth-efficient constant-envelope DPSK modulation/demodulation scheme which can be applied to non-linear TDMA communication systems. Some specific contributions are summarized below.

* Introduction of Nyquist pulse shapes to improve the bandwidth efficiency of differential PSK signals while the envelope is kept constant.
* Analytical derivations of power spectral density functions and performance of differential PSK signals in an AWGN environment.
* Analysis of the effect of the low-pass filter on the performance given that

input noise to this filter is not additive and not Gaussian. This analysis can be applied to any linear system where its input is any kind of random process.

CHAPTER TWO

BANDWIDTH-EFFICIENT CONSTANT-ENVELOPE DPSK MODULATION/DEMODULATION TECHNIQUES

The primary objective of bandwidth-efficient modulation methods is to maximize the bandwidth efficiency, defined as the ratio of data rate to channel bandwidth (measured in bits/s/Hz). In a linear channel, this can be accomplished by filtering. In nonlinear channels, some modulation schemes as Offset quadrature phase shift keying (OQPSK) and minimum shift keying (MSK) can be used to reduce the out-of-band spectral components after filtering.

2.1 The needs of Bandwidth-Efficient Constant-Envelope DPSK Schemes

Transmission of constant envelope signal can reduce distortions introduced by nonlinear channels, and therefore simplify the design of certain elements as the high power amplifier (HPA).

The TDMA transmission technique has been introduced to achieve higher efficiency and flexibility in satellite communication systems. A system model for a conventional satellite circuit is shown in Figure 2.1. The simplified model of a satellite link consists of a transmitting earth station, a satellite transponder, and a receiving earth station. At the transmitting earth station the transmit band pass filter is used to band-limit the spectrum. The high power amplifier (HPA), operated near saturation, creates both AM/AM and AM/PM conversion of the modulated carrier. The satellite input and output multiplex filters are used to

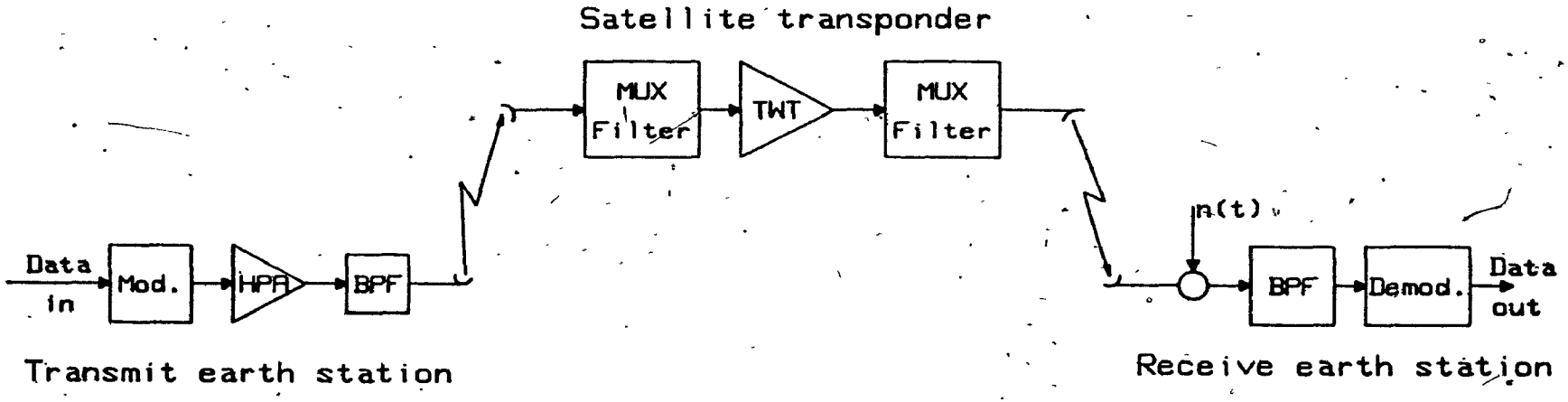

Fig. 2.1 - Communication satellite system model

band-limit the signal and thereby reduce the spectral spreading caused by the TWT. At the receiving earth station, the receive filter is used to band-limit the thermal noise and reduce the adjacent channel interference.

A TDMA scheme requires some form of frame structure and a global timing mechanism to achieve non-overlapping transmission, because in TDMA each outstation is scheduled by the central station to transmit RF burst in short non-overlapping intervals. Each burst generally consists of two parts: the principle part containing the carrier and bit timing recovery (CBR) sequence, and the unique word (UW) to allow the receiver acquisition, the message part to carry traffic data. A typical TDMA frame organization is shown in Figure 2.2.

The frame efficiency of a TDMA system can be defined as the ratio of the number of symbols available for carrying traffic to the total number of symbols available in the TDMA frame

$$\text{TDMA efficiency} = \frac{traffic\ \ bits}{transmission\ \ bits}$$

To increase the TDMA efficiency, the preample should be kept as short as possible, requiring receivers to have fast acquisition. Since TDMA transmitter has only one single carrier, its power amplifier can operate in saturation to maximize its power efficiency. To avoid the spectral regrowth the modulated signals should have a constant envelope [11-12].

In differential phase shift keying (DPSK), there is no need to acquire the synchronous carrier at the receiver. This has several effects when DPSK is used in satellite communication systems. The omission of the carrier recovery circuitry on the satellite means a saving in hardware complexity, reduces risk of failure

CBR : Carrier and clock recovery

UW : Unique word

DATA : Communication channel.

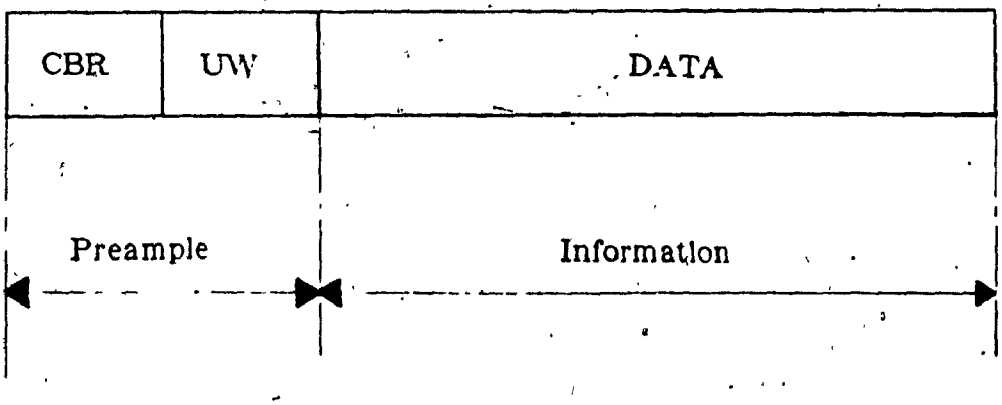

Figure 2.2 - An example of TDMA Frame

and reduces the duration of the preample part, i.e. increases the TDMA efficiency.

2.2 Conventional Differential Phase Shift Keying

Differential phase shift keying is the non-coherent version of the PSK signals. In this technique, it is assumed that there is enough stability in the oscillators and the medium so that there will be negligible abrupt change in phase reference from one information pulse to the next.

Information bits are differentially encoded in terms of the phase change between successive pulses. For example, a 0^o phase shift from the previous pulse could designate Mark, and 180^0 phase shift could designate a Space.

Block diagrams of a conventional DPSK modulator and demodulator are shown in Figure 2.3a and 2.3b, respectively. The differential encoding operation performed by the modulator is explained in Figure 2.4. The encoding process starts with an arbitrary first bit, and there after the encoded bit stream d_k is generated by

$$d_k = \overline{b_k \oplus d_{k-1}} = d_{k-1} b_k \oplus \overline{d_{k-1}}\,\overline{b_k} \tag{2.1}$$

The differential sequence $\{ d_k \}$ is converted into the sequence $\{ a_n \}$. The output of the low-pass filter in Figure 2.3a can be written as

$$m(t) = \sum_{n=-\infty}^{+\infty} a_n h_T(t - nT_b) \tag{2.2}$$

passed through the balanced-modulator gives the DPSK transmitted signal $z(t)$

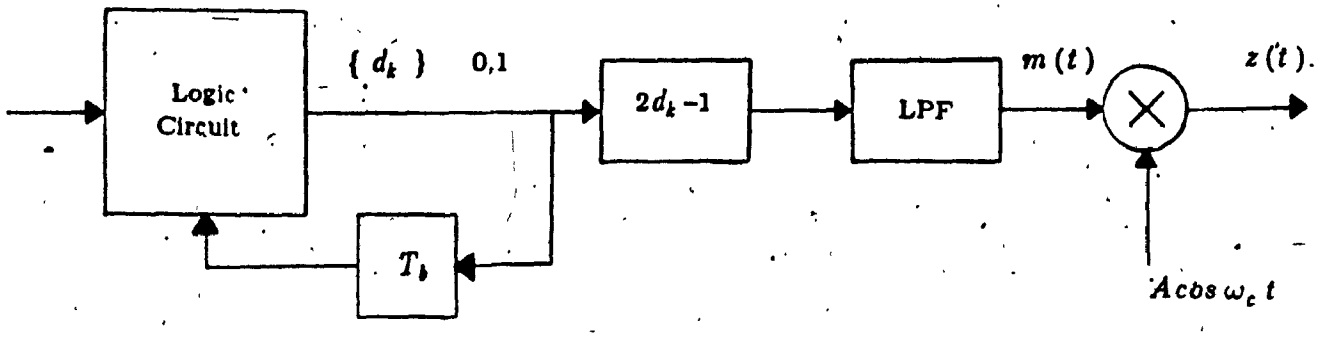

(a)

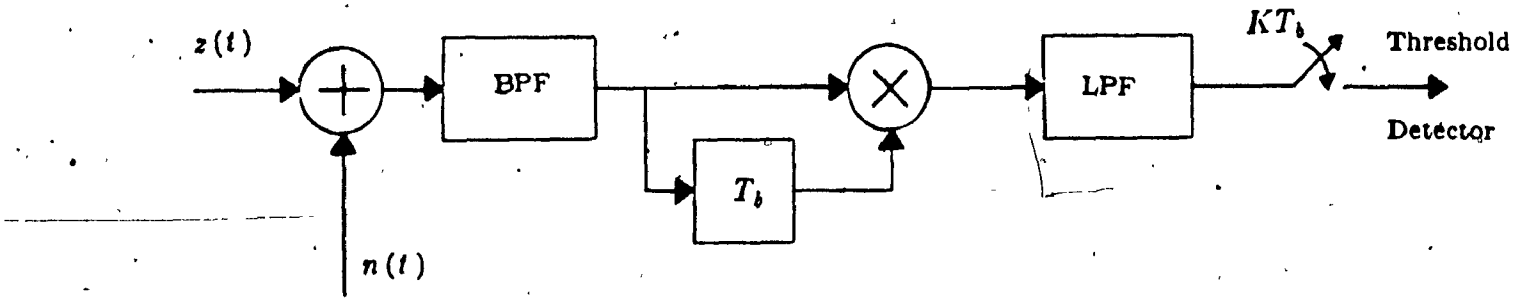

(b)

Figure 2.3 - (a) DPSK Modulator. (b) DPSK Demodulator

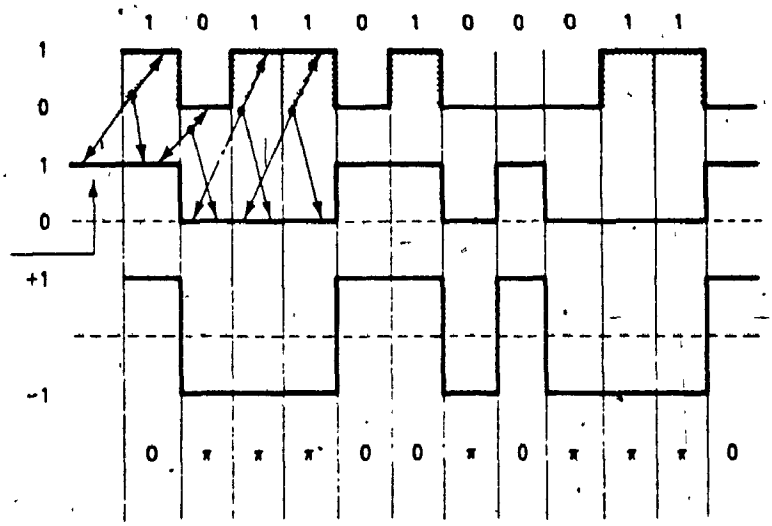

Figure 2.4 - Differential encoding

$$z(t) = Am(t)\cos(2\pi f_c t) \tag{2.3}$$

In this equation $m(t)$ is the modulating signal and $\cos(2\pi f_c t)$ is a carrier signal.

The linear structure of the conventional DPSK signals simplifies the analysis of spectral properties and response behavior to linear systems. As can be seen, the power spectral density of $z(t)$ is simply determined by the Fourier transform of the function $m(t)$.

$$Z(f) = A\left[M(f - f_c) + M(f + f_c)\right] \tag{2.4}$$

The shape of the power spectral density of the DPSK signals depends on the shape of the pulse $h_T(t)$. Thus, the spectral properties can be improved by using bandwidth-efficient pulse shape $h_T(t)$.

Analyzing equation (2:3), the function $z(t)$ appear to be an *amplitude-modulated* wave with envelope $m(t)$ and carrier signal $\cos(2\pi f_c t)$. The shape of the envelope $m(t)$ of the modulated carrier depends on the shape of the pulse $h_T(t)$. To improve the spectral properties of $z(t)$, the pulse shape $h_T(t)$ should be bandlimited. Unfortunately, this introduces more envelope fluctuation which implies high spectral regrowth after a non-linear amplifier.

It is now obvious that the modem of Figure 2.3 is limited, there is no way to improve the bandwidth of the transmitted signal without an envelope distortion since the transmitted signal has a constant envelope only when the wave shape $h_T(t)$ is a rectangular pulse of duration T_b.

At the receiver, the decoding process can be accomplished without a coherently recovered carrier, because the digital information had been differentially encoded

in the carrier phase at the transmitter. The output of the predetection band-pass filter is assumed to be the transmitted signal $z(t)$ plus additive noise

$$r(t) = Am(t)\cos(2\pi f_c t) + n(t) \tag{2.5}$$

The receive detector measures the phase difference between two successive signaling intervals.

$$r_1(t) = A\cos(2\pi f_c t + \phi_1) + n_1(t) \tag{2.6}$$

and

$$r_2(t) = A\cos(2\pi f_c t + \phi_2) + n_2(t) \tag{2.7}$$

Since the noise signal $n(t)$ can be represented in the form

$$n(t) = n_c(t)\cos(2\pi f_c t + \phi) + n_s(t)\sin(2\pi f_c t + \phi) \tag{2.8}$$

the phase between $r_1(t)$ and $r_2(t)$ may be expressed as

$$\Delta\phi = \phi_2 - \phi_1 + \tan^{-1}\left(\frac{n_{s1}}{A + n_{c1}}\right) - \tan^{-1}\left(\frac{n_{s2}}{A + n_{c2}}\right) \tag{2.9}$$

If two successive transmitted bits are the same, an error is committed when the differential phase due to noise

$$\Delta\phi_N = \tan^{-1}\left(\frac{n_{s1}}{A + n_{c1}}\right) - \tan^{-1}\left(\frac{n_{s2}}{A + n_{c2}}\right)$$

exceeds 90^0. It can be shown [27] that an exact expression for the probability of

bit error in this case is

$$P_e = \frac{1}{2} e^{-\frac{A^2}{N_0}} \tag{2.10}$$

We notice here that the analysis for the probability of error is done only at the output of the phase comparator. A perfect channel and an appropriate transmit pulse shape $p(t)$ were assumed to obtain zero intersymbol interference at the phase comparator output. In a more general model, low-pass filter is included to limit the noise effects. This low-pass filter is required to determine the right filter. In the following, we introduce a modem for bandwidth-efficient constant-envelope DPSK signals. In this modem not only the envelope is kept constant but the spectral properties of the DPSK signals are also improved with respect to the conventional ones by band-limited *phase* pulse shapes. Low-pass filter at the receiver to keep zero intesymbol interference and to improve the performance are also investigated.

2.3 Bandwidth-Efficient Constant-Envelope Differential PSK

Figure 2.5 shows the block diagram of a generalized M-ary DPSK modulator/demodulator (modem). The concept was introduced in [2] to generate a bandwidth-efficient, constant envelope, multi-level DPSK signals. Only binary DPSK is considered in this thesis.

As shown in Figure 2.6, the binary data sequence $\{ a_n \}$, where $a_n = \pm 1$ is converted into a phase difference sequence and passed through a filter to form phase difference signal $\Delta\phi(t)$. The phase $\phi(t)$ is formed as

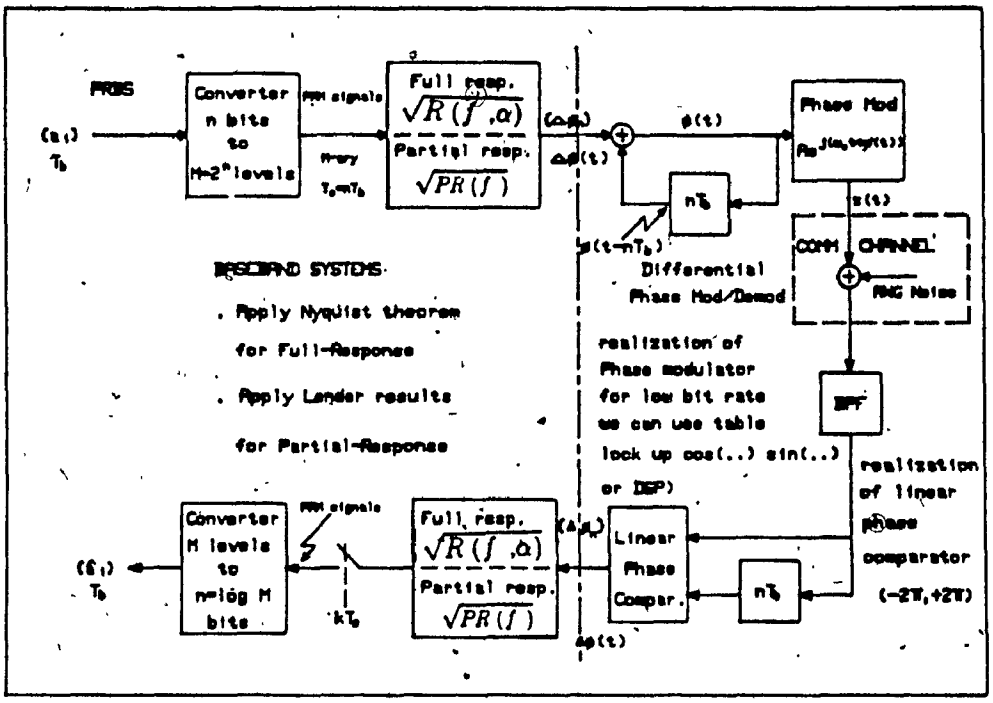

Figure 2.5

"SERIALLY DIFFERENTIAL DEMODULATION"

for M-ary DPSK (full/partial response)

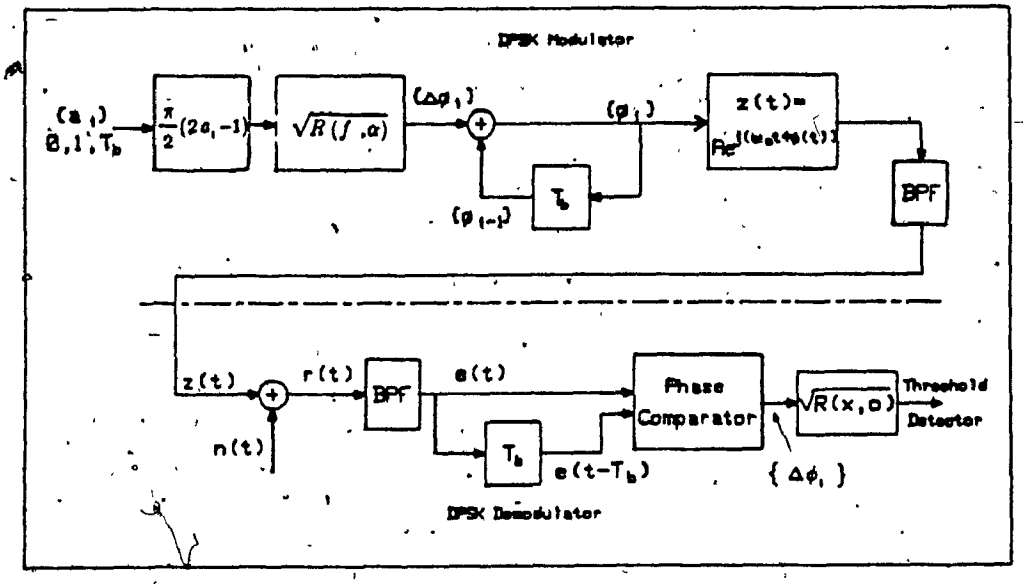

Figure 2.6 - Binary DPSK Modulator/Demodulator

$$\phi(t) = \Delta\phi(t) + \phi(t - T_b) \tag{2.11}$$

and can be represented as

$$\phi(t) = \frac{\pi}{2} \sum_{n=-\infty}^{+\infty} p(t - nT_b , \underline{a}_n) \tag{2.12}$$

$$\underline{a}_n = (\ldots, a_{n+1}, a_n, a_{n-1}, \cdots)$$

where T_b is the bit time interval corresponding to the input sequence $\{ a_n \}$ that has been converted to the NRZ sequence $\{ \pm 1 \}$. The function $p(t - nT_n , \underline{a}_n)$ is a pulse of duration T_b whose peak amplitude and shape depend on the wave shape $h_T(t)$ and may depend on the value of the sequence a_n.

$$p(t - nT_b , \underline{a}_n) = \sum_{i=-\infty}^{+\infty} a_{n-i} h_T(t - (n - i)T_b), \qquad 0 \leq t - nT_b \leq T_b \tag{2.13}$$

The phase $\phi(t)$ modulates a carrier and produces the phase shift-keyed (PSK) signal given by

$$z(t) = Ae^{j(2\pi f_c t + \phi(t))} \tag{2.14}$$

where A is the constant amplitude and f_c is the carrier frequency

The amplitude of the DPSK transmitted signal $z(t)$ is always constant. Using this property, we can choose the pulse shape $h_t(t)$ to improve the bandwidth-efficiency of the DPSK signal.

The power spectral density in this case is not easily found, because this angle modulation is a nonlinear process and the spectrum components of the modulated waveform are directly related to the message spectrum. The system

complexity is compensated for by improved bandwidth-efficiency and signal-to-noise ratio at the receiver output without having to increase the transmitted power.

The average power in the DPSK modulated signal is easily computed from equation (2.14). Multiplying (2.14) by its complex conjugate and taking the time-average yields

$$P_a = \frac{1}{T_b} \int_0^{T_b} |z(t)|^2 dt = \frac{1}{T_b} \int_0^{T_b} A^2 dt$$

which gives

$$P_a = A^2 \tag{2.15}$$

Thus, the power contained in the output of the DPSK modulator is independent of the message signal.

The output of the predetection band-pass filter is assumed to be the modulated carrier $z(t)$ plus additive white noise

$$e(t) = z(t) + n(t) = Ae^{j(2\pi f_c t + \phi(t))} + n(t) \tag{2.16}$$

the signal $e(t)$ and the one-bit delayed version of itself $e(t - T_b)$ are passed through a phase comparator to reproduce the information in form of phase difference. The output of the phase comparator is passed through a low-pass filter and then compared with zero, a decision is made in favor of one or zero depending whether the low pass filter output is + or -, respectively. The DPSK demodulator will be described in more details in Chapter 3 with an analysis for the

probability of error.

In the absence of noise, the transfer function of the system reduces to

$$F(f) = H_T(f)H_R(f) = H(f) \tag{2.17}$$

where the transmit and receive filters are equally split for a maximum signal-to-noise ratio, i.e.

$$H_T(f) = H_R(f) = \sqrt{H(f)}$$

and its impulse response is given by

$$h(t) = h_T(t) * h_R(t) \tag{2.18}$$

The design of a binary data transmission system consists of specifying the pulse shapes $h_T(t)$ and $h_R(t)$ to minimize the combined effects of intersymbol interference (ISI) and noise in order to achieve a minimum probability of error for given data rate and power levels in the system.

The intersymbol interference can be eliminated by proper choice of the equivalent pulse shape $h(t)$. For a zero ISI, $h(t)$ should satisfy

$$h(nT_b) = \begin{cases} 1 & \text{for } n = 0 \\ 0 & \text{for } n \neq 0 \end{cases} \tag{2.19}$$

and

$$\sum_{k=-\infty}^{+\infty} H(f + \frac{k}{T_b}) = T_b \qquad \text{for } |f| \leq \frac{1}{2T_b} \tag{2.20}$$

where $H(f)$ is the Fourier transform of $h(t)$.

The condition given in equation (2.20) is called the Nyquist (pulse shaping) criterion. A computer-generated eye diagram [26] for the raised cosine pulse with a roll-off factor of $\alpha = 0.3$ is shown in Figure 2.7.

The transmitted pulse shape $h_T(t)$ considered in this thesis is the impulse response of the square root of the raised cosine filter $\sqrt{R(f\ ,\alpha)}$.

$$h_T(t) = r(t\ ,\alpha) \tag{2.21}$$

and

$$\sqrt{R(f\ ,\alpha)} = \begin{cases} \sqrt{T_b}, & |f\ | \leq (1-\alpha) f_0 \\ \sqrt{T_b}\cos\left[\dfrac{\pi}{4\alpha f_0}(|f\ | - (1-\alpha) f_0)\right] & (1-\alpha) f_0 \leq |f\ | \leq (1+\alpha) f_0 \\ 0, & \textit{elsewhere} \end{cases} \tag{2.22}$$

where

$$f_0 = \frac{1}{2T_b} \tag{2.23}$$

Taking the Fourier inverse transform of equation (3.21) (Appendix A), we get

$$r(t\ ,\alpha) = \frac{\sin\left[\pi(1-\alpha)x\right]}{x\,\pi\sqrt{T_b}} + \frac{4\alpha}{\pi\sqrt{T_b}\left(1-(4\alpha x)^2\right)}\left[\cos\left[(1+\alpha)\pi x\right] + 4\alpha x \sin\left[(1-\alpha)\pi x\right]\right]. \tag{2.24}$$

where

$$x = 2f_0 t \tag{2.25}$$

Plots of $\sqrt{R(f\ ,\alpha)}$ and $r(t\ ,\alpha)$ for three values of the parameter α are shown in Figure 2.8, it can be seen that for $\alpha = 0$, $\sqrt{R(f\ ,\alpha)}$ represents the ideal Nyquist filter. Since $\sqrt{R(f\ ,\alpha)}$ is band-limited, its inverse transform $r(t\ ,\alpha)$ is time-unlimited. In order to compute the power spectral density (PSD), the pulse $r(t,\alpha)$ should be truncated in the time domain, which can be done by multiplying the wave shape $h_t(t)$ given by equation (2.15) by a rectangular pulse of duration KT_b, where K is an an integer from 0 to $+\infty$.

In the next Chapter, the power spectral density of DPSK signals will be derived and the effect of truncated $r(t\ ,\alpha)$ on the spectral properties will be examined.

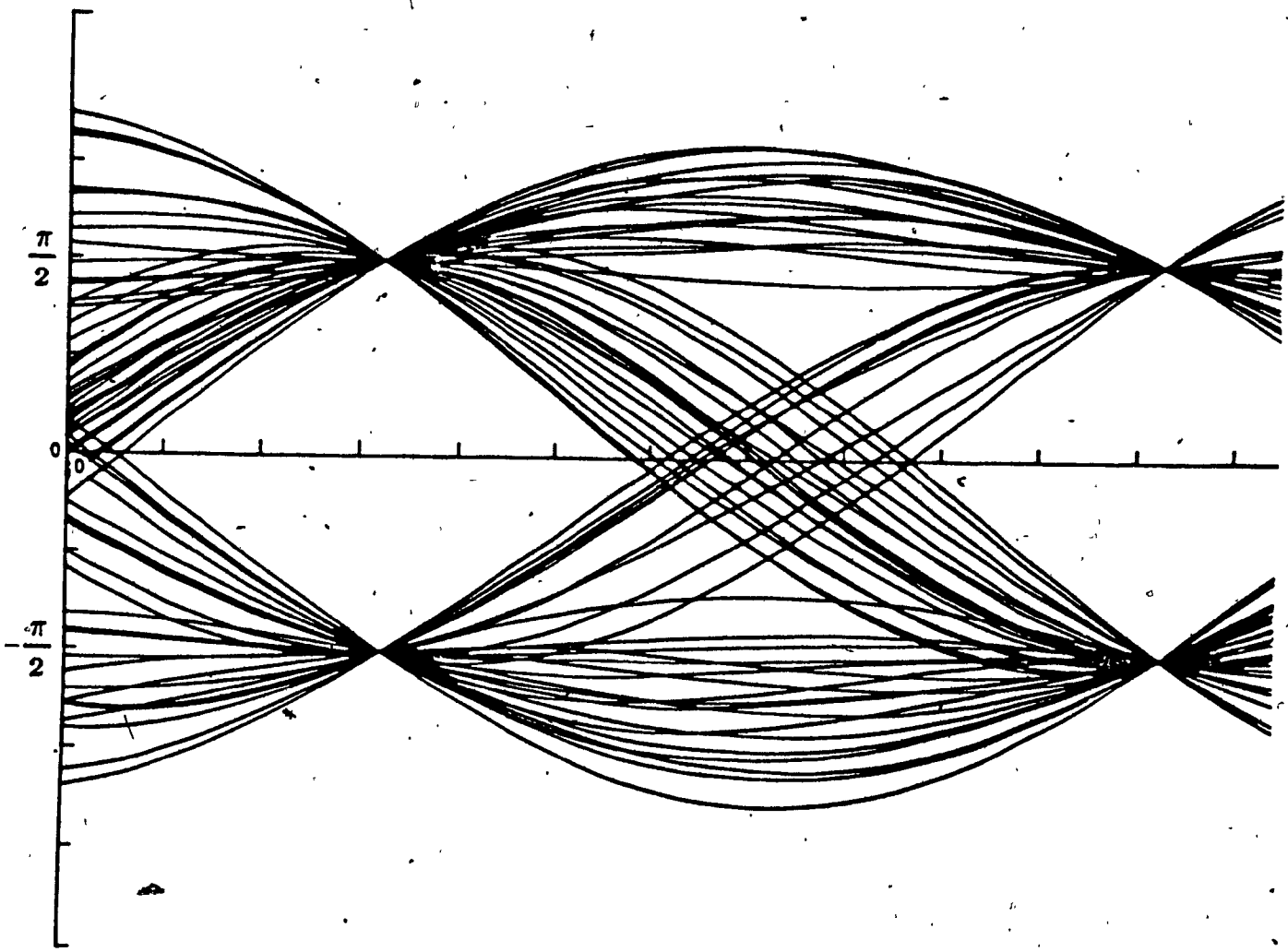

Figure 2.7

A computer-generated eye diagram for the raised cosine pulse with a roll-off factor of $\alpha = .3$

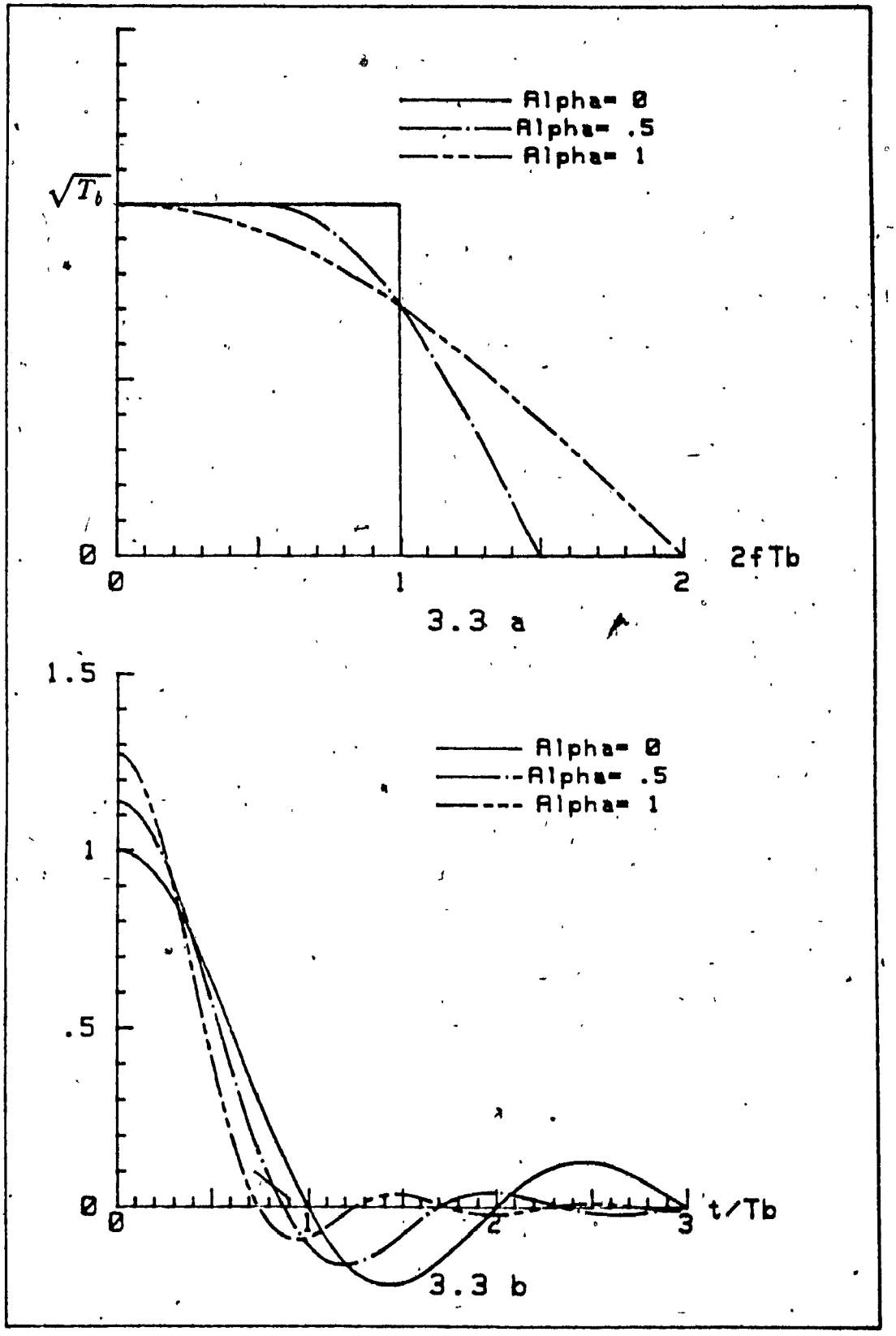

Figure 2.8 - Square root of the Nyquist filter

(a) Transfer function. (b) Impulse response

CHAPTER THREE

SPECTRAL PROPERTIES OF BANDWIDTH-EFFICIENT CONSTANT ENVELOPE DPSK SIGNALS

3.1 Power Spectral Density Function of the DPSK Signal

The DPSK signal is given by the complex representation as

$$z(t) = s(t)\, e^{j(2\pi f_c t)} \tag{3.1}$$

where

$$s(t) = Ae^{j\phi(t)} \tag{3.2}$$

which is called the *complex envelope* of $z(t)$.

It is well known that [19]

$$Z(f) = S(f - f_c) \tag{3.3}$$

where $Z(f)$ and $S(f)$ are the power spectral densities of $z(t)$ and $s(t)$ respectively.

The above relation indicates that it is sufficient to derive $S(f)$ since $Z(f)$ is just a translation in the frequency domain of $S(f)$.

Subdividing the time axis into an infinite number of bit interval $\left[(n-1)T_b\ ,\ nT_b\right]$ where n is an integer from $-\infty$ to $+\infty$, the complex envelope

can be rewritten as

$$s(t) = A \sum_{n=-\infty}^{+\infty} b(t - nT_b \ , \underline{a}_n) \tag{3.4}$$

where $Ab(t - nT_b \ , \underline{a}_n)$ is the portion of $s(t)$ defined in the n^{th} time interval $\left[(n-1)T_b \ , nT_b \right]$.

From the expression of $\phi(t)$ given by equation (3.1)

$$b(t - nT_b \ , \underline{a}_n) = \exp\left[j\frac{\pi}{2} \sum_{i=-\infty}^{+\infty} a_{n-i} \, h_T \left(t - (n-i)T_b \right) \right] \tag{3.5}$$

$$\text{for } 0 \leq t - nT_b \leq T_b$$

The process $s(t)$ is cyclostationary, i.e. $s(t)$ is periodic in time domain with period T_b. The autocorrelation function of $s(t)$ is also periodic with the same period T_b, i.e.

$$R_s(\tau) = \frac{1}{T_b} \int_0^{T_b} R_s(t + \tau \ , t) dt \tag{3.6}$$

where

$$R_s(t + \tau, t) = E\left[s(t + \tau) s^*(t) \right] \tag{3.7}$$

Substituting the expression of $s(t)$ given by equation (3.4) into the above equation, $R_s(\tau)$ can be rewritten as

$$R_s(\tau) = \frac{A^2}{T_b} \sum_{n=-\infty}^{+\infty} \sum_{k=-\infty}^{+\infty} \int_0^{T_b} b(t + \tau - nT_n \ , \underline{a}_n) b^*(t - kT_b \ , \underline{a}_k) dt \tag{3.8}$$

let

$$x = t - kT_b \quad , \quad i = n - k \tag{3.9}$$

After changing the variables, equation (3.9) becomes

$$R_s(\tau) = \frac{A^2}{T_b} \sum_{n=-\infty}^{+\infty} \sum_{k=-\infty}^{+\infty} \int_{-kT_b}^{(1-k)T_b} \overline{b(x + \tau - iT_b \ , \underline{a}_{i+k}) b^*(x \ , \underline{a}_k)} dx \tag{3.10}$$

Since the symbols are stationary, the pair of vectors $(\underline{a}_{i+k} \ , \underline{a}_k)$ can be replaced by the pair of vectors $(\underline{a}_i \ , \underline{a}_0)$.

Equation (3.10) becomes

$$R_s(\tau) = \frac{A^2}{T_b} \sum_{i=-\infty}^{+\infty} \sum_{k=-\infty}^{+\infty} \int_{-kT_b}^{(1-k)T_b} \overline{b(x + \tau - iT_b \ , \underline{a}_i) b^*(x \ , \underline{a}_0)} dx \tag{3.11}$$

Equation (3.11) indicates that the summation over k of the segmented integrals is a single integral over all possible values of the variable x from $-\infty$ to $+\infty$. The autocorrelation function can be rewritten as

$$R_s(\tau) = \frac{A^2}{T_b} \sum_{i=-\infty}^{+\infty} \int_{-\infty}^{+\infty} \overline{b(t + \tau - iT_b \ , \underline{a}_i) b^*(t \ , \underline{a}_0)} dt \tag{3.12}$$

The power spectral density (PSD) function $S(f)$ is given by the Fourier transform of the autocorrelation function $R_s(\tau)$.

$$S(f) = \int_{-\infty}^{+\infty} R_s(\tau) e^{-j2\pi f \tau} d\tau$$

$$= \frac{A^2}{T_b} \sum_{i=-\infty}^{+\infty} \int_{-\infty}^{+\infty} \int_{-\infty}^{+\infty} \overline{b(t+\tau-iT_b, \underline{a}_i) b^*(t, \underline{a}_0)} e^{-j2\pi f \tau} dt d\tau \quad (3.13)$$

Interchanging the order of the Fourier transform and the statistical average, this becomes

$$S(f) = \frac{A^2}{T_b} \sum_{i=-\infty}^{+\infty} E\left[\int_{-\infty}^{+\infty} e^{-j2\pi f t} \int_{-\infty}^{+\infty} b(\tau, \underline{a}_i) e^{-j2\pi f \tau} d\tau\, b^*(t, \underline{a}_0) dt \right] e^{-j2\pi f i T_b}$$

$$= \frac{A^2}{T_b} \sum_{i=-\infty}^{+\infty} E\left[\int_{-\infty}^{+\infty} b(t, \underline{a}_i) e^{-j2\pi f t} dt \int_{-\infty}^{+\infty} b^*(t, \underline{a}_0) e^{j2\pi f t} dt \right] e^{-j2\pi f i T_b} \quad (3.14)$$

Let $B(f, \underline{a}_i)$ defined as the the Fourier transform of the function $b(t, \underline{a}_i)$. The function $S(f)$ becomes

$$S(f) = \frac{A^2}{T_b} \sum_{i=-\infty}^{+\infty} \overline{B(f, \underline{a}_i) B^*(f, \underline{a}_0)} e^{-j2\pi f i T_b}$$

$$= \frac{A^2}{T_b} \sum_{i=-\infty}^{+\infty} S_{b,i}(f) e^{-j2\pi f i T_b} \quad (3.15)$$

where

$$S_{b,i}(f) = \overline{B(f, \underline{a}_i) B^*(f, \underline{a}_0)} \quad (3.16)$$

Equation (3.16) can also be written as [2]

$$S_{b,i}(f) = \int_{-\infty}^{+\infty} \int_{-\infty}^{+\infty} \overline{b(t, \underline{a}_i) b^*(t', \underline{a}_0)} e^{-j2\pi f(t-t')} dt dt'$$

$$= \int_{-\infty}^{+\infty} \int_{-\infty}^{+\infty} R_{b,i}(t, t') e^{-j2\pi f(t-t')} dt dt' \qquad (3.17)$$

where

$$R_{b,i}(t, t') = \overline{b(t, \underline{a}_i) b^*(t', \underline{a}_0)} \qquad (3.18)$$

which is the autocorrelation function of $b(t, \underline{a}_i)$.

From equation (3.5) we notice that the duration of $b(t, \underline{a}_i)$ is T_b, we can write (3.17)

$$S_{b,i}(f) = \int_0^{T_b} \int_0^{T_b} R_{b,i}(t, t') e^{-j2\pi f(t-t')} dt dt' \qquad (3.19)$$

To compute the power spectral density $S(f)$, we need only the terms with non-negative indices because, from equation (3.16) and the stationarity of symbols

$$S_{b,-i}(f) = \overline{B(f, \underline{a}_{-i}) B^*(f, \underline{a}_0)} = \overline{B(f, \underline{a}_0) B^*(f, \underline{a}_i)}$$

$$= \overline{\left[B(f, \underline{a}_i) B^*(f, \underline{a}_0)\right]^*} = \overline{\left[B(f, \underline{a}_i) B^*(f, \underline{a}_0)\right]}^*$$

$$= S_{b,i}^*(f) \qquad (3.20)$$

and

$$S_{b,0}(f) = \overline{|B(f, \underline{a}_0)|^2} \qquad (3.21)$$

which shows that the power spectral density $S(f)$ is a continuous and real function of frequency.

$$S(f) = S_{b,0}(f) + 2\sum_{i=1}^{+\infty} \mathrm{Re}\left[S_{b,i}(f)e^{-j2\pi f iT_b}\right] \tag{3.22}$$

Equation (3.22) presents the power spectral density of the DPSK signal for an infinite wave shape. In order to compute $S(f)$, the shaping function has to be truncated specially when numerical computations are required.

3.2 Shaping Function having Finite Time Duration

If the duration of the wave shape is KT_b where K is a positive integer, then for $|i| \geq K$ the set of symbols a_i and a_0 becomes independent. The function $S_{b,i}(f)$ given by equation (3.16) can be written as

$$\begin{aligned} S_{b,i}(f) &= \overline{B(f, \underline{a}_i)}\,\overline{B^*(f, \underline{a}_0)} \\ &= \overline{B(f, \underline{a}_i)}\left[\overline{B(f, \underline{a}_0)}\right]^* \qquad \text{for } |i| \geq K \end{aligned} \tag{3.23}$$

Since the symbols are stationary, the vector $\underline{a}_i$ can be replaced by the vector $\underline{a}_0$ to give

$$\begin{aligned} S_i(f) &= \overline{B(f, \underline{a}_0)}\left[\overline{B(f, \underline{a}_0)}\right]^* \\ &= \left|\overline{B(f, \underline{a}_0)}\right|^2 \qquad \text{for } |i| \geq K \end{aligned} \tag{3.24}$$

The total power density function becomes

$$S(f) = \frac{A^2}{T_b} \sum_{i=-K+1}^{K-1} \left[S_{b,i}(f) - S_{b,K}(f) \right] e^{-j2\pi f i T_b}$$

$$+ \frac{A^2}{T_b} S_{b,K}(f) \sum_{i=-\infty}^{+\infty} e^{-j2\pi f i T_b} \tag{3.25}$$

Note that

$$\sum_{i=-\infty}^{+\infty} e^{-j2\pi f i T_b} = \frac{1}{T_b} \sum_{i=-\infty}^{+\infty} \delta(f - \frac{i}{T_b}) \tag{3.26}$$

which is the sum of discrete spectral lines.

The power spectral density $S(f)$ has a continuous part $S_c(f)$ and a discrete part $S_d(f)$, i.e.

$$S(f) = S_c(f) + S_d(f) \tag{3.27}$$

The continuous part $S_c(f)$ is given by

$$S_c(f) = \frac{A^2}{T_b} \sum_{i=-K+1}^{K-1} \left[S_{b,i}(f) - S_{b,K}(f) \right] e^{-j2\pi f i T_b}$$

$$= \frac{A^2}{T_b} \left\{ S_{b,0}(f) - S_{b,K}(f) \right\}$$

$$+ \frac{2A^2}{T_b} \sum_{i=1}^{K-1} \mathrm{Re} \left[\left[S_{b,i}(f) - S_{b,K}(f) \right] e^{-j2\pi f i T_b} \right] \tag{3.28}$$

And the discrete part $S_d(f)$ is given by

$$S_d(f) = \left(\frac{A}{T_b}\right)^2 S_{b,K}(f) \sum_{i=-\infty}^{+\infty} \delta\left(f - \frac{i}{T_b}\right)$$

$$= \left(\frac{A}{T_b}\right)^2 \sum_{i=-\infty}^{+\infty} S_{b,K}\left(\frac{i}{T_b}\right)\delta\left(f - \frac{i}{T_b}\right) \qquad (3.29)$$

The wave shape $h_T(t)$ is symmetric, hence $S_{b,K}\left(\frac{i}{T_b}\right) = 0$ and $S_d(f) = 0$, i.e. $S(f)$ is continuous in the frequency domain (see equation (3.22)).

3.2.1 Shaping Function of Duration T_b

When the duration of the wave shape is T_b, no overlap exists between pulses. All the symbols are independent. Using equation (3.5), we get

$$b(t, a_i) = e^{j\frac{\pi}{2} a_n h_T(t)}, \qquad 0 \leq t \leq T_b \qquad (3.30)$$

And

$$S_{b,0}(f) = \overline{|B(f, a_0)|^2} \qquad (3.31)$$

Using the autocorrelation function, $S_{b,0}$ becomes

$$S_{b,0}(f) = \int_0^{T_b} \int_0^{T_b} R_{b,0}(t, t') e^{-j2\pi f(t-t')} dt dt' \qquad (3.32)$$

But $R_{b,0}(t, t')$ is defined as

$$R_{b,0}(t\ ,t'\ ) = \overline{b\,(t\ ,a_0)b^*(t'\ .,a_0)}$$

$$= \cos\left[\frac{\pi}{2}\left(h_T(t\,) - h_T(t'\ )\right)\right] \qquad (3.33)$$

Combining equations (3.32) and (3.33), we get

$$S_{b,0}(f\ ) = \int_0^{T_b}\int_0^{T_b} \cos\left[\frac{\pi}{2}\left(h_T(t\,) - h_T(t'\ )\right)\right] e^{-j\,2\pi f\,(t\,-\,t'\,)}dtdt'$$

$$= \left|\ \int_0^{T_b} cos\,(\frac{\pi}{2}h_T(t\,))e^{-j\,2\pi f t}\,dt\ \right|^2$$

$$+\ \left|\ \int_0^{T_b} sin\,(\frac{\pi}{2}h_T(t\,))e^{-j\,2\pi f t}\,dt\ \right|^2 \qquad (3.34)$$

And

$$S_{b,1}(f\ ) = |\,\overline{B(f\ ,a_0}\,|^2$$

$$) = \left|\ \int_0^{T_b} cos\,(\frac{\pi}{2}h_T(t\,))e^{-j\,2\pi f t}\,dt\ \right|^2 \qquad (3.35)$$

Hence, the total power density function will be given by

$$S(f\ ) = \frac{A^2}{T_b}\left|\ \int_0^{T_b} sin\,(\frac{\pi}{2}h_T(t\,))e^{-j\,2\pi f t}\,dt\ \right|^2 \qquad (3.36)$$

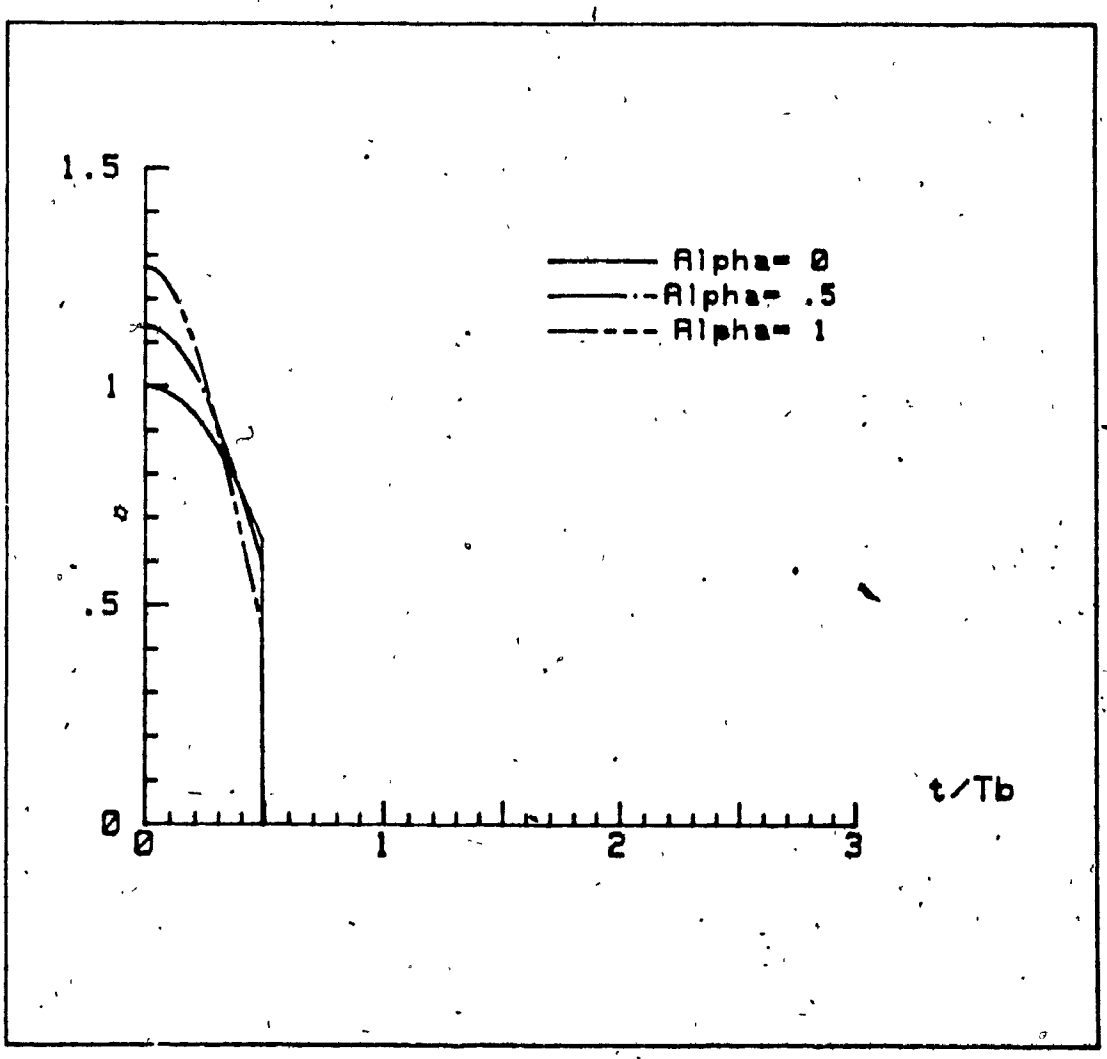

Fig. 3.1 - Shaping Function of Duration Tb

3.2.2 Shaping Function of duration $2T_b$

Using the same procedure, the power density function is given by

$$S(f) = \frac{A^2}{T_b}\left\{S_{b,0}(f) - S_{b,2}(f)\right\}$$

$$+ 2\frac{A^2}{T_b}\mathrm{Re}\left[\left(S_{b,1}(f) - S_{b,2}(f')\right)e^{-j2\pi f T_b}\right] \tag{3.37}$$

where

$$S_{b,0}(f) = |Z_1(f)|^2 + |Z_2(f)|^2 + |Z_3(f)|^2 + |Z_4(f)|^2 \tag{3.38}$$

$$S_{b,1}(f) = |Z_1(f)|^2 + Z_2(f)Z_3^*(f) \tag{3.39}$$

$$S_{b,2}(f) = |Z_1(f)|^2 \tag{3.40}$$

with

$$Z_1(f) = F\left[\cos\left(\frac{\pi}{4}h_{T0}(t)\right)\cos\left(\frac{\pi}{4}h_{T1}(t)\right)\right] \tag{3.41}$$

$$Z_2(f) = F\left[\cos\left(\frac{\pi}{4}h_{T0}(t)\right)\sin\left(\frac{\pi}{4}h_{T1}(t)\right)\right] \tag{3.42}$$

$$Z_3(f) = F\left[\sin\left(\frac{\pi}{4}h_{T0}(t)\right)\cos\left(\frac{\pi}{4}h_{T1}(t)\right)\right] \tag{3.43}$$

$$Z_4(f) = F\left[\sin\left(\frac{\pi}{4}h_{T0}(t)\right)\sin\left(\frac{\pi}{4}h_{T1}(t)\right)\right] \tag{3.44}$$

and

$$h_{T0}(t) = h_T(t)\Pi\left(\frac{t + T_b/2}{T_b}\right) \tag{4.45}$$

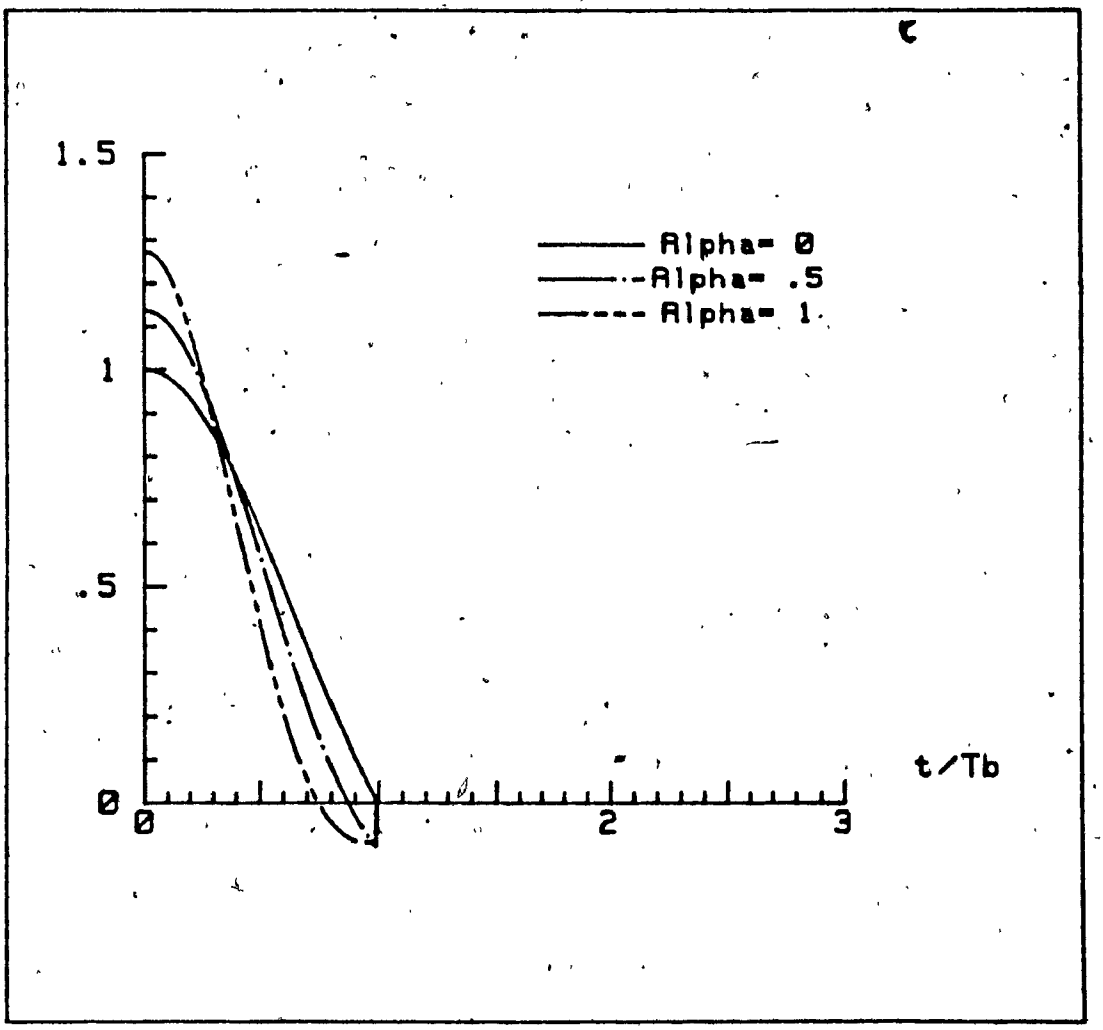

Fig. 3.2 - Shaping Function of Duration 2Tb

$$h_{T1}(t) = h_T(t)\Pi\left(\frac{t - T_b/2}{T_b}\right) \tag{3.46}$$

3.2.3 Shaping Function of Duration KT_b

The wave shape $h_T(t)$ is split into K pulses of duration T_b each. These pulses are given by

$$h_{Ti}(t) = h_T(t + iT_b)\Pi\left(\frac{t + KT_b}{T_b}\right), \qquad i = 0,1,\ldots,K-1 \tag{3.47}$$

From equation (3.5), the function $b(t, \underline{a}_i)$ is

$$b(t, \underline{a}_i) = \exp\left(j\frac{\pi}{2}\sum_{n=0}^{K-1} a_{i-n}\, h_{Tn}(t)\right)$$

$$= \prod_{n=0}^{K-1} \exp\left(j\frac{\pi}{2} a_{i-n}\, h_{Tn}(t)\right) \tag{3.48}$$

The statistical average of $b(t, \underline{a}_i)$ is given by

$$m_b(t) = \prod_{n=0}^{K-1} E\left\{\exp\left(j\frac{\pi}{2} a_{i-n}\, h_{Tn}(t)\right)\right\}$$

$$= \prod_{n=0}^{K-1} \cos\left(\frac{\pi}{2} h_{Tn}(t)\right) \tag{3.49}$$

let define

$$m_{b,i}(t) = \cos\left(\frac{\pi}{2} h_{Ti}(t)\right) \tag{3.50}$$

The autocorrelation function of $b(t, \underline{a}_i)$ is given by

$$R_{b,i}(t\ ,\ t'\ ) = E\left[b\,(t\ ,\ \underline{a}_i)b^{*}(t'\ ,\ \underline{a}_0)\right]$$

$$= E\left[\prod_{n=0}^{K-1}\prod_{l=0}^{K-1}\exp\left\{\,j\frac{\pi}{2}(a_{i-n}\,h_{Tn}(t) - a_{i-l}\,h_{Tl}(t'\ ))\right\}\right] \quad (3.51)$$

Based on the independence of some symbols on each other, the autocorrelation function can be written in the equivalent form [19]

$$R_{b,i}(t\ ,\ t'\ ) = E\left[\prod_{k=0}^{i-1} e^{\,j\frac{\pi}{2}a_k\,h_{Tk}(t)}\prod_{k=i}^{i-1} e^{\,j\frac{\pi}{2}a_k\,(h_{Tk}(t) - h_{T(i-i)}(t'\ ))}\prod_{k=i}^{K-1} e^{\,j\frac{\pi}{2}a_k\,h_{Tk}(t'\ )}\right]$$

$$= \prod_{k=0}^{i-1} m_{b,k}(t)\prod_{k=i}^{K-1}\phi_{k,k-i}(t\ ,\ t'\ )\prod_{k=i}^{K-1} m_{b,k}(t'\ ) \quad (3.52)$$

where $m_{b,k}(t)$ is as defined in equation (3.50) and

$$\phi_{i,j}(t\ ,\ t'\ ) = \cos\left[\frac{\pi}{2}(h_{Ti}(t) - h_{Tj}(t'\ ))\right] \quad (3.53)$$

And

$$S_{b,i}(f\ ) = \int_0^{T_i}\int_0^{T_i} R_{b,i}(t\ ,\ t'\ )e^{-j\,2\pi f\,(t\ -\ t'\ )}dtdt' \quad (3.54)$$

The power density function can be easily found using equation (3.28)

$$S(f) = \frac{A^2}{T_b}\left\{S_{b,D}(f) - S_{b,K}(f)\right\}$$

$$+ 2\frac{A^2}{T_b}\mathrm{Re}\left[\sum_{i=1}^{K-1}(S_{b,i}(f) - S_{b,K}(f))e^{-j2\pi f iT_b}\right] \qquad (3.55)$$

3.3 Numerical results

In this chapter we presented all the derivations for the power spectral density of constant envelope PSK signals. With some modifications, this method can be applied in the case of M-ary DPSK signal, e.g. instead of T_b we will have $T_s = kT_b$, and instead of $M = 2$ we will have $M = 2^k$. The shape of the power spectral density may look like the shape of the spectra for the the binary case with a narrower bandwidth.

The power spectral density shown in the next figures are calculated with numerical integration using discrete Fourier transform (DFT). Figures 3.4 to 3.8 show the power spectral density for the square root of the raised cosine pulse of duration T_b, $2T_b$, $3T_b$, $4T_b$ and $5T_b$ respectively. It is obvious that the $5T_b$ pulse is much better than the T_b and $2T_b$ pulses for all values of α. The main lobe is almost the same but the side lobes become lower as the number of T_b increases.

It is also noted from Figure 3.9 that the power spectrum is approximatly the same for pulses of duration $4T_b$ and $5T_b$, the wave shape of duration $5T_b$ can represent the case when the wave shape is time-unlimited ($K \rightarrow +\infty$), i.e the power spectral density of the DPSK signal.

Figure 3.10 illustrates a comparison between DPSK, Offset QPSK and MSK

signals. Although Offset QPSK and MSK belong to quadrature modulation family, the binary DPSK offer almost the main-lobe and a lower high-order side-lobes than these signals. These results give a promissing future for high-level DPSK signals.

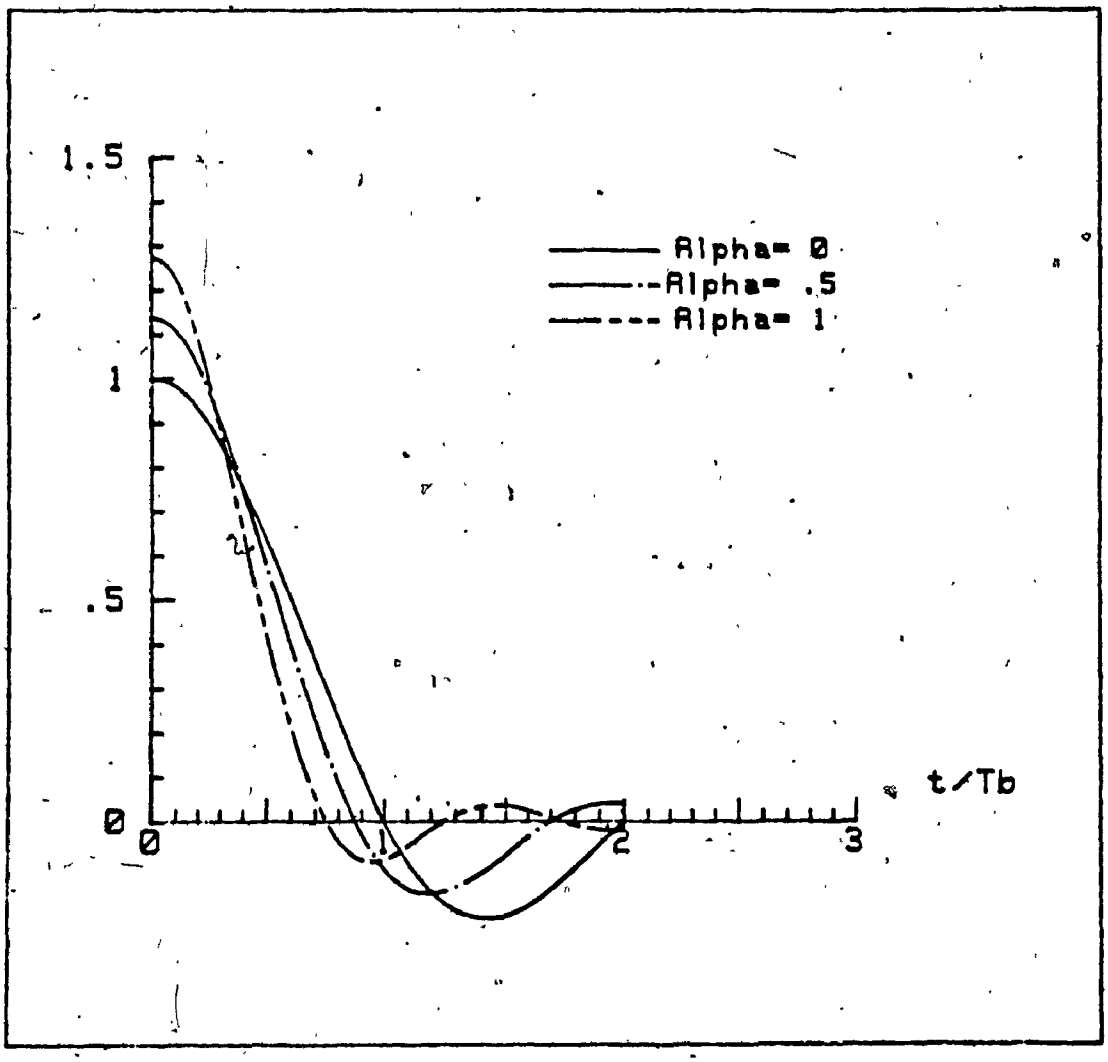

Fig. 3.3 - Shaping Function of Duration 4Tb

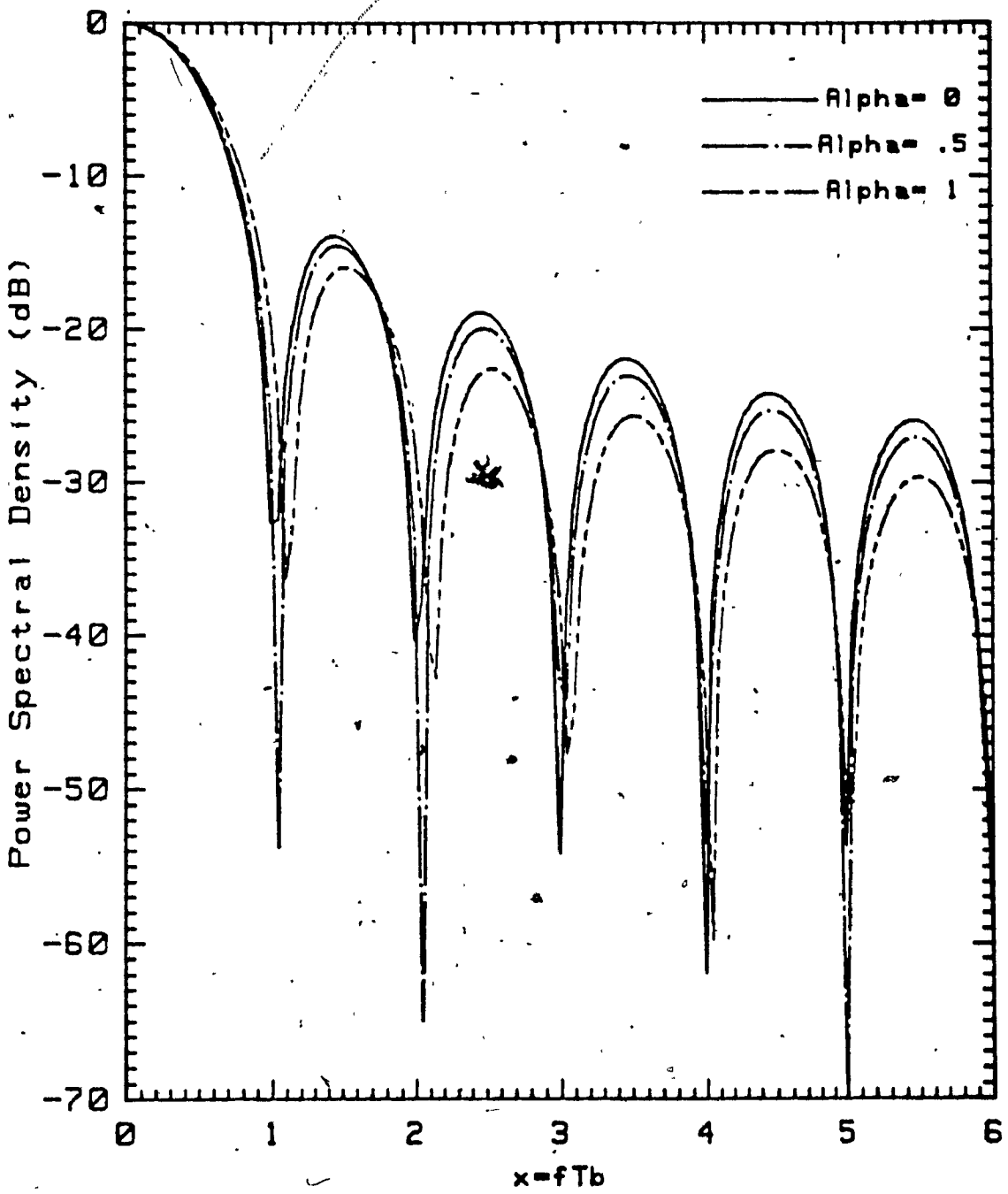

Fig. 3.4 - Shaping function of duration Tb

Sqrt raised cosine pulse

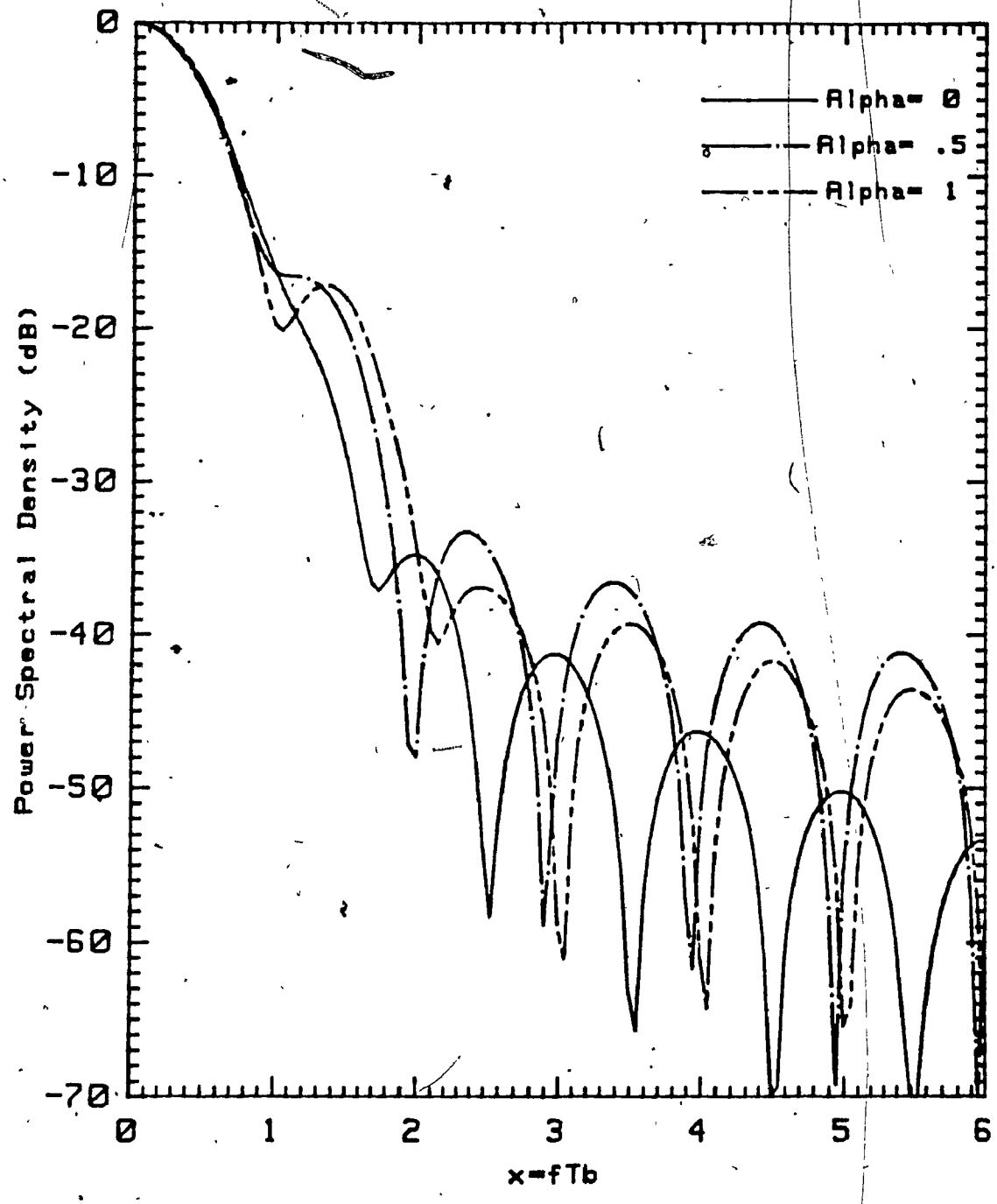

Fig. 3.5 - Shaping function of duration 2Tb

Sqrt Raised cosine pulse

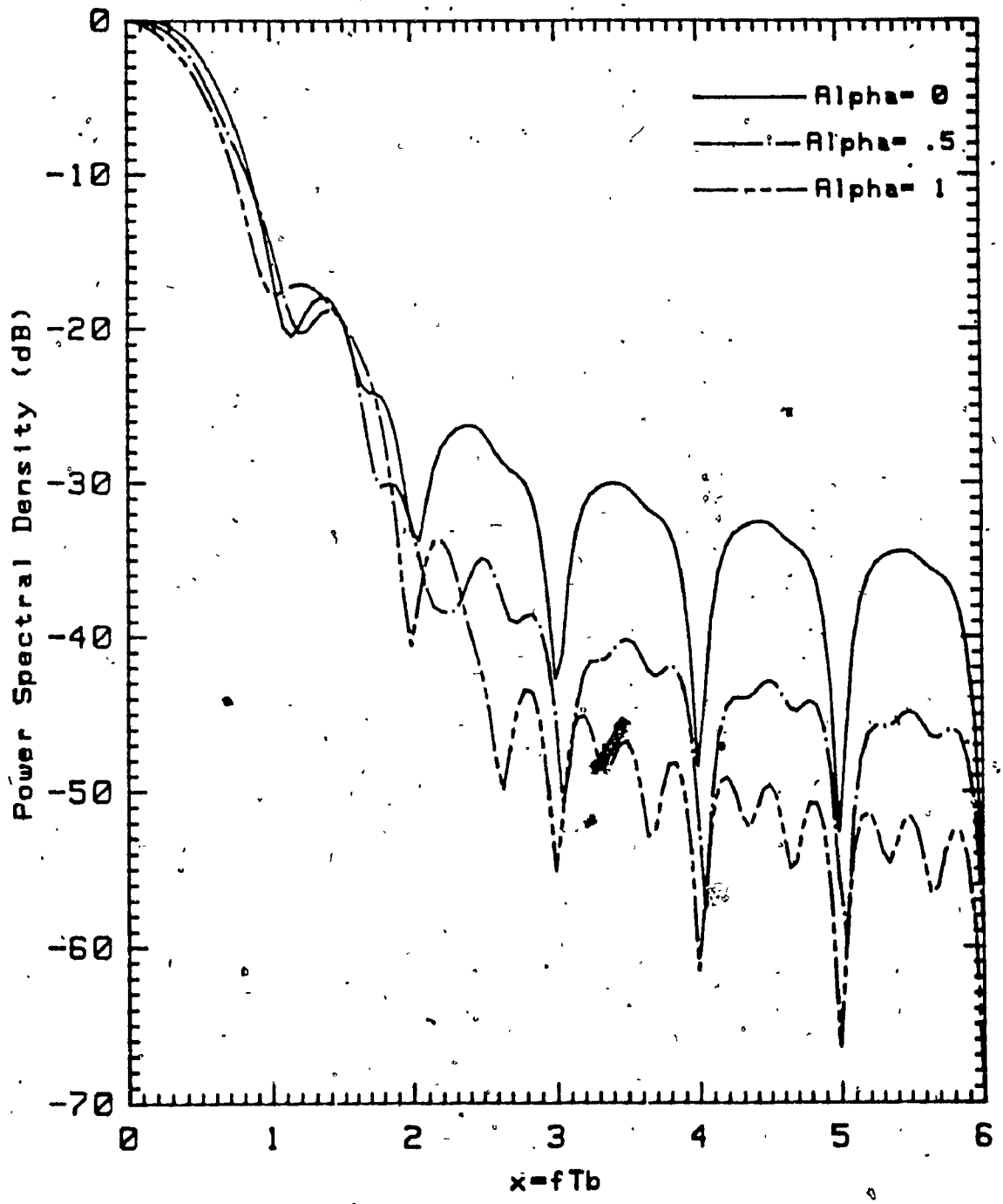

Fig. 3.6 - Shaping function of duration 3Tb

Sqrt Raised cosine pulse

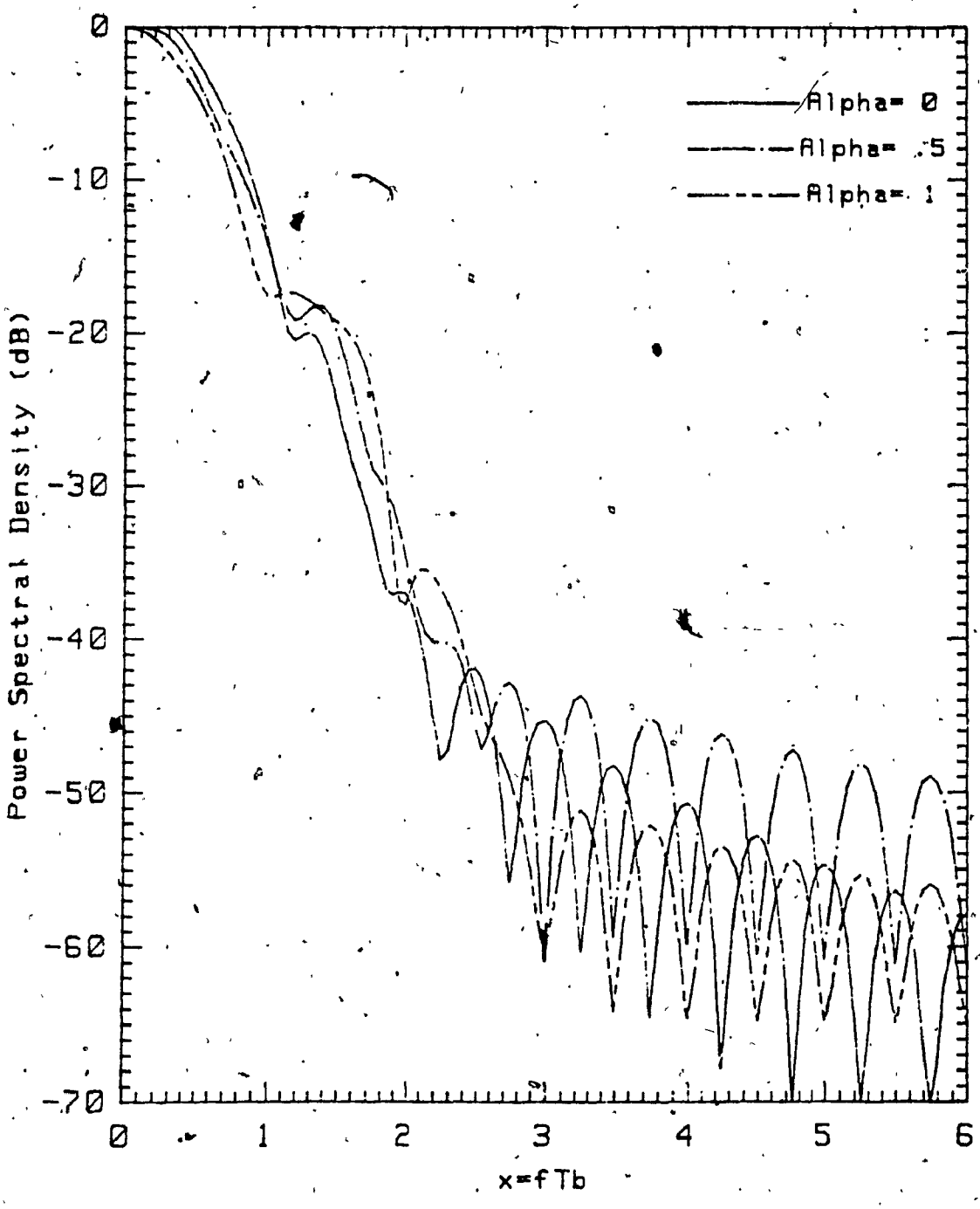

Fig. 3.7 - Shaping function of duration 4Tb

Sqrt raised cosine pulse

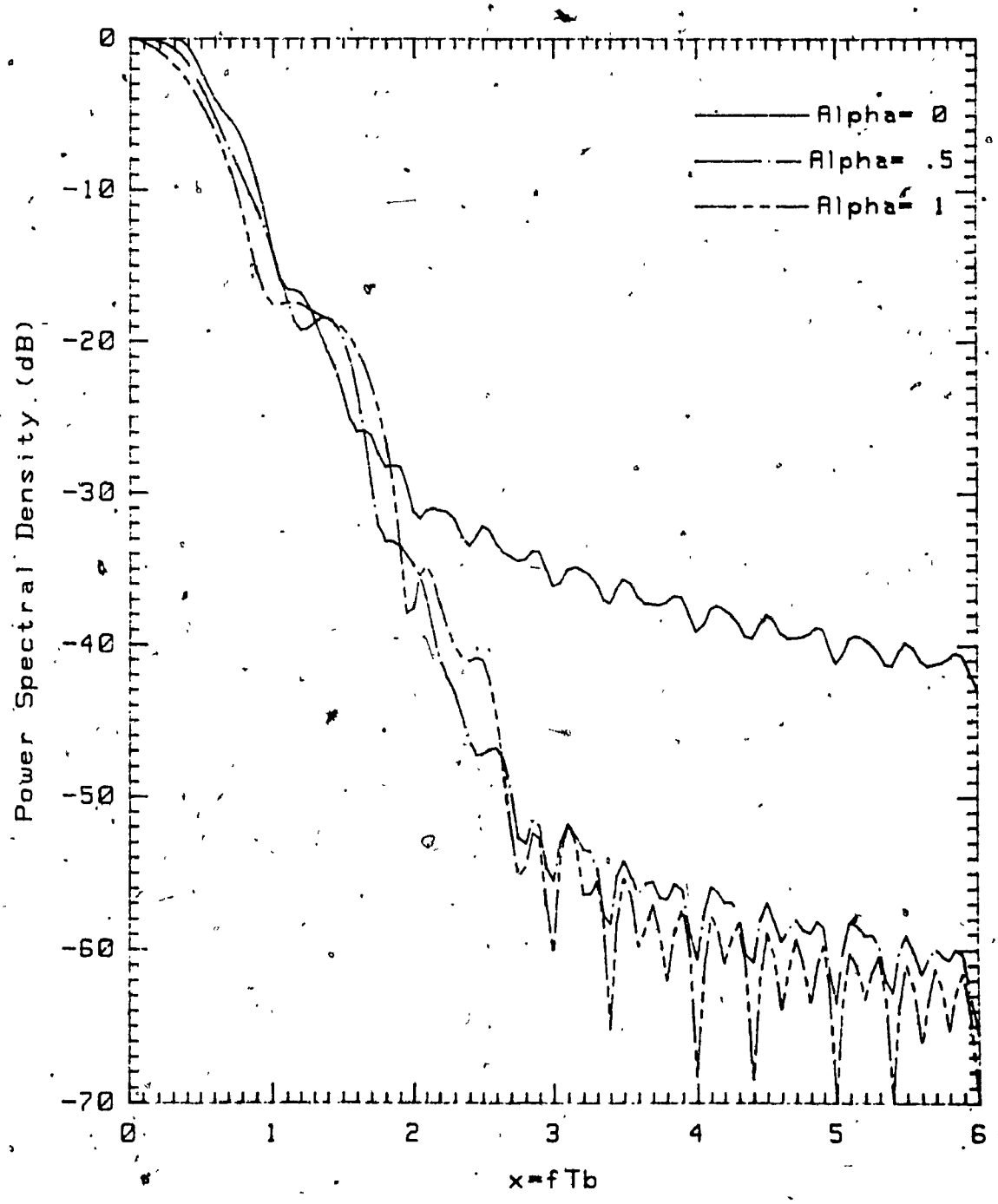

Fig. 3.8 - Shaping function of duration 5Tb

Sqrt raised cosine pulse

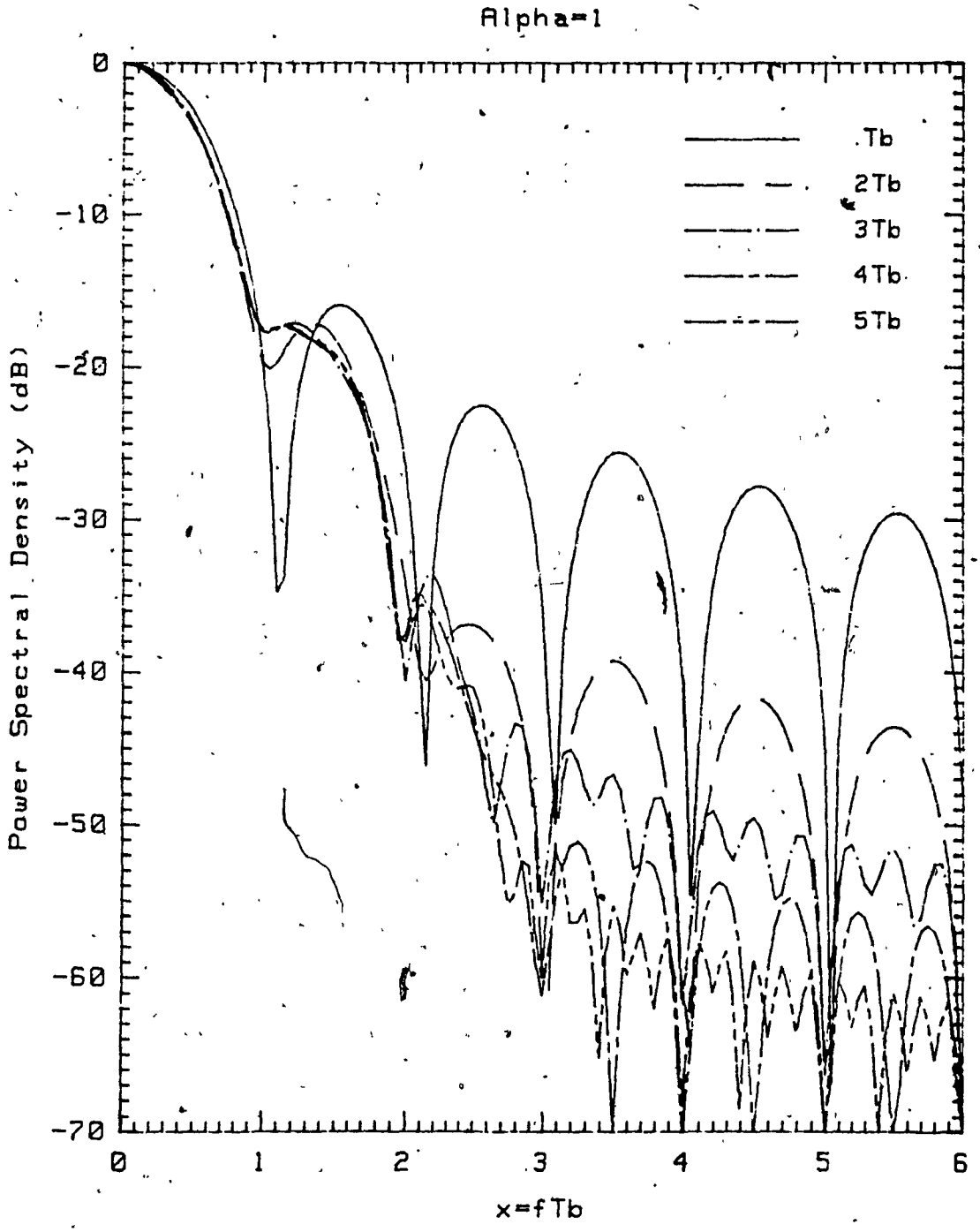

Fig. 3.9 - Shaping function of duration 5Tb

Sqrt raised cosine pulse

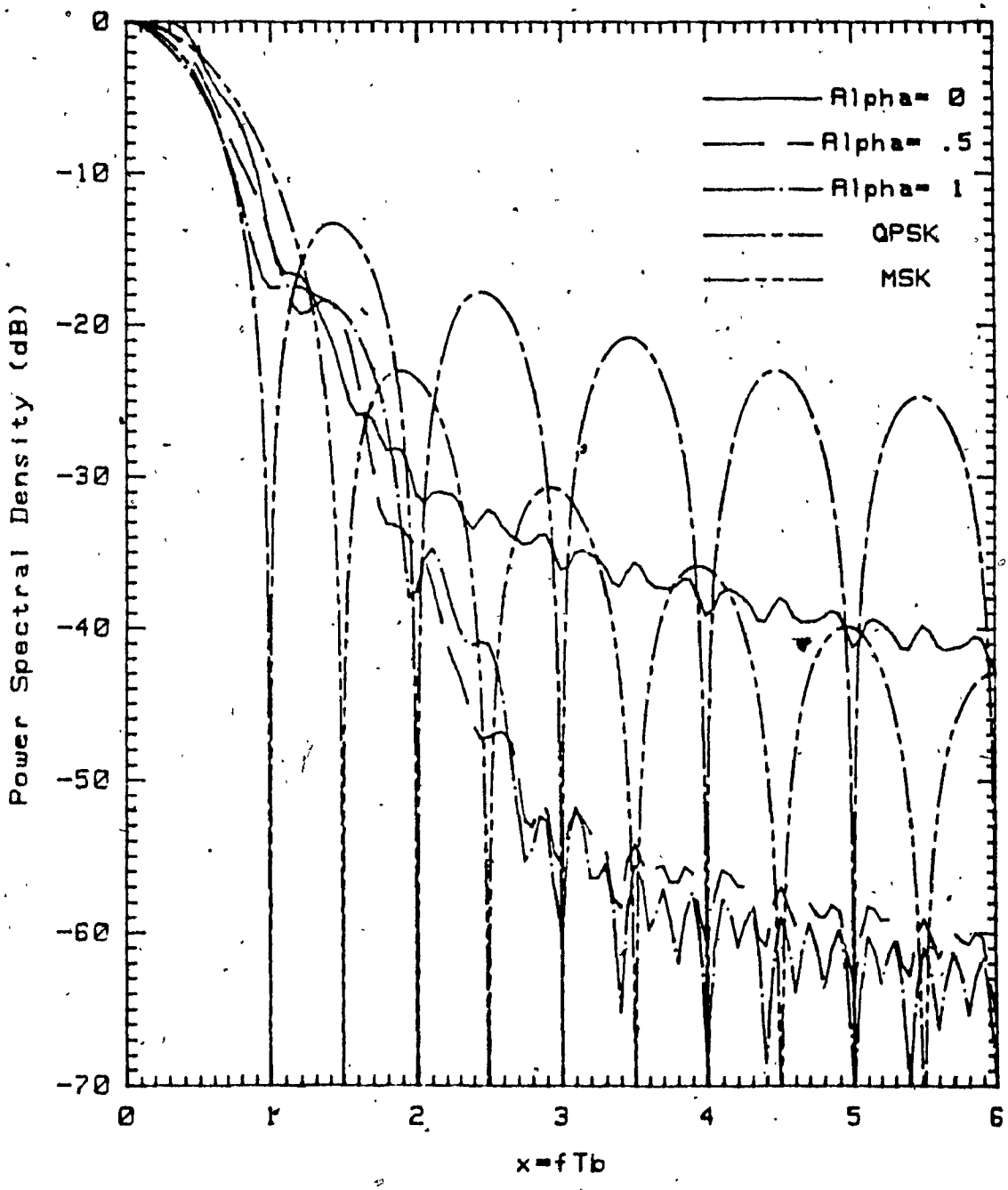

Fig. 3.10 - Shaping function of duration 5Tb

Comparison with other PSD

CHAPTER FOUR

PERFORMANCE OF CONSTANT ENVELOPE DPSK SIGNALS

In the DPSK demodulation scheme, the phase reference for demodulation is derived from the phase of the carrier of the preceding signaling interval, and the receiver decodes the digital information based on the phase difference.

The noise performance of the DPSK might appear to be inferior compared to coherent PSK because the phase reference is contaminated by noise in the DPSK scheme. In the following we will derive an expression for the probability of error for the DPSK scheme and discuss the effect of some elements on the performance of the system.

Consider the system shown in Figure 4.1. The output of the predetection band pass filter is assumed to be the modulated carrier $z(t)$ plus additive noise

$$e(t) = z(t) + n(t) = Ae^{j(2\pi f_c t + \phi(t))} + n(t) \qquad (4.1)$$

where A is the amplitude per channel, f_c is the carrier frequency and $\phi(t)$ is defined by equation (2.12).

For the transmission bandwidth smaller than the carrier frequency, f_c, the noise $n(t)$ can represented as

$$n(t) = \left[n_c(t) + jn_s(t)\right] e^{j2\pi f_c t} \qquad (4.2)$$

BPF: band pass filter

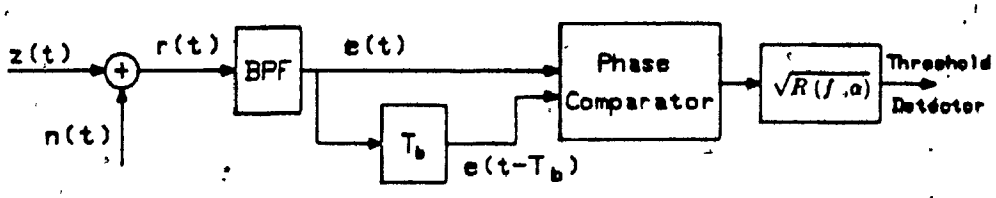

Fig. A.1 – Linear DPSK detector

where $n_c(t)$, $n_s(t)$ are additive white noise with power spectral density $N_0/2$.

For a wide bandwidth, the output of the predetection band-pass filter can be written as

$$e(t) = Ae^{j(2\pi f_c t + \phi(t))} + \left[n_c(t) + jn_s(t)\right] e^{j2\pi f_c t} \tag{4.3}$$

where

$$\overline{n_c^2} = \overline{n_s^2} = \frac{N_0}{2} \tag{4.4}$$

Equation (4.3) can be written

$$e(t) = \left[Ae^{j\phi(t)} + n_c(t) + jn_s(t)\right] e^{j2\pi f_c t} \tag{4.5}$$

Without loss of generality, we consider the complex envelope of $e(t)$

$$\rho(t) = \left[A\cos\phi(t) + n_c(t)\right] + j\left[A\sin\phi(t) + n_s(t)\right]$$

$$= \rho_c(t) + j\rho_s(t) \tag{4.6}$$

$\rho_c(t)$, $\rho_s(t)$ are Gaussian random processes with mean $A\cos\phi(t)$ and $A\sin\phi(t)$ respectively, and variance $N_0/2$.

At the sampling points, kT_b, the sampled values of the angle $\phi(t)$ is $\phi(kT_b) = +\pi$ or 0 with probability of 1/2. Therefore

$$A\cos\phi(kT_b) = \pm A \qquad \text{with probability of } 1/2$$

$$A\sin\phi(kT_b) = 0$$

The phase comparator provides the angle between two successive vectors $\rho(kT_b)$ and $\rho([k-1]T_b)$, i.e.

$$\Delta\phi_k \triangleq arg\left\{\rho(kT_b)\,,\,\rho\left([k-1]T_b\right)\right\} \tag{4.7}$$

where

$$\rho(kT_b) = \left[\pm A + n_c(kT_b)\right] + jn_s(kT_b) \tag{4.8}$$

and

$$\rho\left([k-1]T_b\right) = \left[\pm A + n_c\left([k-1]T_b\right)\right] + jn_s\left([k-1]T_b\right) \tag{4.9}$$

Without noise components $n_c(t)$ and $n_s(t)$, $\Delta\phi_k$ takes the value of 0 if $\rho(kT_b)$ and $\rho\left([k-1]T_b\right)$ have the same values or π if $\rho(kT_b)$ and $\rho\left([k-1]T_b\right)$ have the different values, i.e.

$$\Delta\phi_k = \begin{cases} 0, & \rho(kT_b).\rho\left([k-1]T_b\right) = A^2 \\ \pi, & \rho(kT_b).\rho\left([k-1]T_b\right) = -A^2 \end{cases} \tag{4.10}$$

Note that $\Delta\phi_k = 0$ when the transmitted bit $b_k = 1$ and $\Delta\phi_k = \pi$ when the transmitted bit $b_k = -1$.

In the presence of noise components $n_c(t)$ and $n_s(t)$, the decision boundary is $\pi/2$. The decision rule will be

$$\Delta\phi_k \underset{b_k=1}{\overset{b_k=-1}{\lessgtr}} \frac{\pi}{2} \tag{4.11}$$

In both cases, it can be seen that an error is made if and only if the *absolute* value of $\Delta\phi_k$ is greater than $\pi/2$, independent of the values of the *noise-free* vectors $\rho(kT_b)$ and $\rho\left([k-1]T_b\right)$. Therefore, in computing the probability of error we can consider the simplified case in which the transmitter sends the same waveform, i.e. the received complex envelope is

$$\rho(t) = \left[A + n_c(t)\right] + jn_s(t)$$

$$= A + \eta(t)e^{j\theta(t)} \tag{4.12}$$

where

$$\eta(t) = \sqrt{n_c^2(t) + n_s^2(t)}$$

and

$$\theta(t) = \tan^{-1}\left[\frac{n_s(t)}{n_c(t)}\right].$$

A phase diagram for the vector $\rho(t)$ is shown in Fig. 4.2. Decision regions are not preassigned regions in the observation space, where each region is associated with a particular message point as in coherent detection. Instead, the decision is based on the phase difference between successively received signals.

Two successively received complex envelopes have the form

$$\rho_1(t) = \left[A + n_{c\,1}(t)\right] + jn_{s\,1}(t) \tag{4.13}$$

and

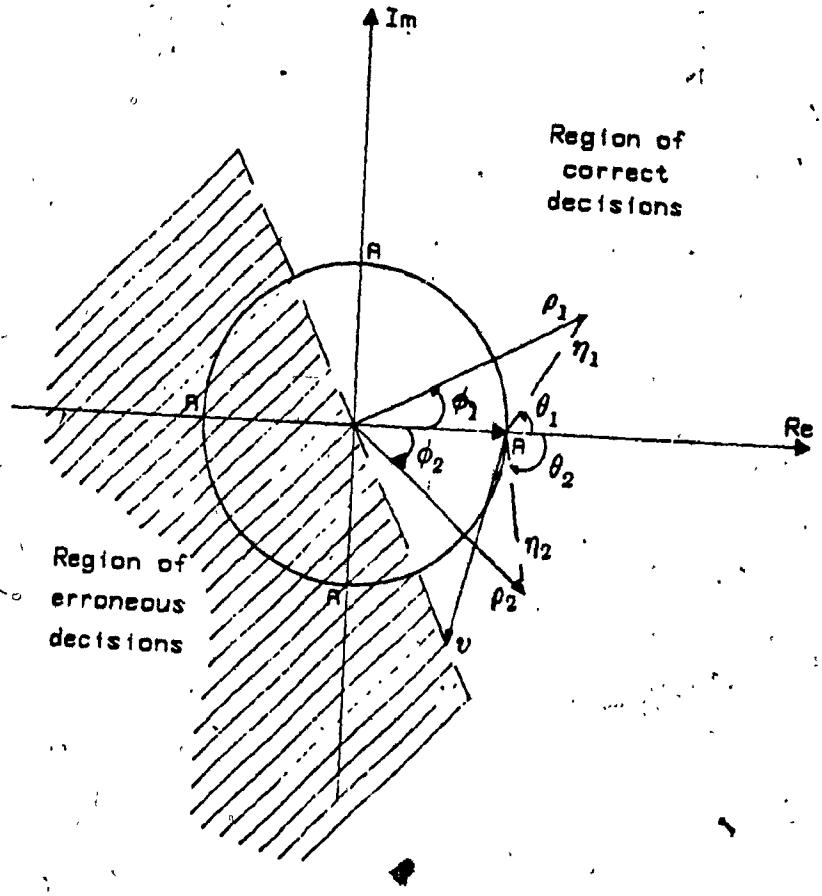

Fig.4.2 - Signal space diagram for DPSK

$$\rho_2(t) = \left[A + n_{c\,2}(t)\right] + jn_{s\,2}(t) \tag{4.14}$$

Let the angle ϕ_1 denotes the phase perturbation produced by the noise vector $n_{c\,1}(t) + jn_{s\,1}(t)$. The angle ϕ_2 denotes the phase perturbation produced by the noise vector $n_{c\,2}(t) + jn_{s\,2}(t)$. The two angles ϕ_1 and ϕ_2 are shown in Fig. 4.2. Based on the decision rule given by equation (4.11), an erroneous decision will be made if and only if

$$\left|\phi_2 - \phi_1\right| > \frac{\pi}{2} \tag{4.15}$$

To use this criteria, it is necessary to find the probability density function of the random variable $\Delta\phi$. Since ϕ_1 and ϕ_2 are i.i.d random variables, the probability density function of $\Delta\phi$ is related to the probability density function of ϕ_1 by the relation

$$f_{\Delta\phi}(\theta) = \int_{-\pi}^{+\pi} f_{\phi_1}(\phi + \theta) f_{\phi_1}(\phi)\, d\phi \tag{4.16}$$

4.5 The Probability Density Function of The Angle Φ_1

We have

$$\phi_1 = \tan^{-1}\left(\frac{n_{s\,1}}{A + n_{c\,1}}\right) \tag{4.17}$$

Its characteristic function is

$$\Phi_{\Phi_1}(\omega) = \frac{1}{\pi N_0} \int_{-\infty}^{+\infty} \int_{-\infty}^{+\infty} e^{j\omega \tan^{-1}\left(\frac{x}{A+y}\right)} e^{-\frac{1}{N_0}(x^2+y^2)}\, dx\, dy \tag{4.18}$$

let

$$x = r\cos\theta - A$$

and

$$y = r\sin\theta$$

Changing the variables in equation (4.18) gives

$$\Phi_{\Phi_1}(\omega) = \int_0^{+\infty} \int_{-\pi}^{+\pi} \frac{r}{\pi N_0} e^{j\omega\theta} \exp\left[-\frac{1}{N_0}\left((r\cos\theta - A)^2 + r^2\sin^2\theta\right)\right] dr\,d\theta \tag{4.19}$$

Rearranging terms, we get

$$\Phi_{\Phi_1}(\omega) = \int_{-\pi}^{+\pi} e^{j\omega\theta} \int_0^{+\infty} \frac{r}{\pi N_0} \exp\left[-\frac{1}{N_0}\left((r - A\cos\theta)^2 + A^2\sin^2\theta\right)\right] dr\,d\theta \tag{4.20}$$

But, we know by definition that

$$\Phi_{\Phi_1}(\omega) = \int_{-\pi}^{+\pi} e^{j\omega\theta} f_{\Phi_1}(\theta)\,d\theta \tag{4.21}$$

Comparing the two equations (4.20) and (4.21), the probability density function of the random angle Φ_1 appear to be

$$f_{\Phi_1}(\theta) = \int_0^{+\infty} \frac{r}{\pi N_0} \exp\left[-\frac{1}{N_0}\left((r - A\cos\theta)^2 + A^2\sin^2\theta\right)\right] dr \qquad (4.22)$$

Let

$$x = \frac{r - A\cos\theta}{\sqrt{N_0}} \qquad (4.23)$$

and

$$dx = \frac{dr}{\sqrt{N_0}}$$

Equation (4.22) becomes

$$f_{\Phi_1}(\phi) = \frac{1}{\pi\sqrt{N_0}} e^{-\frac{A^2}{N_0}\sin^2\phi} \int_{-\frac{A}{\sqrt{N_0}}\cos\phi}^{+\infty} \left(x\sqrt{N_0} + A\cos\phi\right) e^{-x^2} dx \qquad (4.24)$$

We note that

$$\int_{-\frac{A}{\sqrt{N_0}}\cos\phi}^{+\infty} x e^{-x^2} dx = \frac{1}{2} e^{-\frac{A^2}{N_0}\cos^2\phi} \qquad (4.25)$$

and

$$\int_{-\frac{A}{\sqrt{N_0}}\cos\phi}^{+\infty} e^{-x^2} dx = \frac{\sqrt{\pi}}{2}\left[1 + erf\left(\frac{A}{\sqrt{N_0}}\cos\phi\right)\right] \qquad (4.26)$$

where

$$erf\,(x) = \frac{2}{\sqrt{\pi}} \int_0^x e^{-x^2} dx$$

Hence, the probability density function of the phase of the received complex envelope DPSK $f_{\Phi_1}(\phi)$ becomes

$$f_{\Phi_1}(\phi) = \frac{1}{2\pi} e^{-\frac{A^2}{N_0}} + \frac{A}{2\sqrt{\pi N_0}} \cos\phi\, e^{-\frac{A^2}{N_0}\sin^2\phi} \left[1 + erf\,(\frac{A}{\sqrt{N_0}}\cos\phi)\right] \qquad (4.27)$$

$$-\pi \leq \phi \leq +\pi$$

The function $f_{\Phi_1}(\phi)$ is plotted in Figure 4.3 for various values of the signal-to-noise ratio $\frac{A^2}{N_0}$.

Given the expression of $f_{\Phi_1}(\phi)$, the integral given by equation (4.16) can not be done without using numerical integration. Figure 4.4 illustrates the probability density function $f_{\Delta\Phi}(\phi)$ for different values of signal-to-noise ratio $\frac{A^2}{N_0}$.

Another method which theoritically will lead to the same result and avoid numerical integrations can be used [22].

Consider the vector presentation given in Figure 4.2, where ρ_1, ρ_2 are two successively received complex envelopes.

Given that the complex envelope ρ_1 was sent, ρ_2 is in error if and only if it lies outside the correct region. Since the message signal is supposed to be constant, an error is caused only by the noise vector η_2. From Figure 4.2, we deduce that an

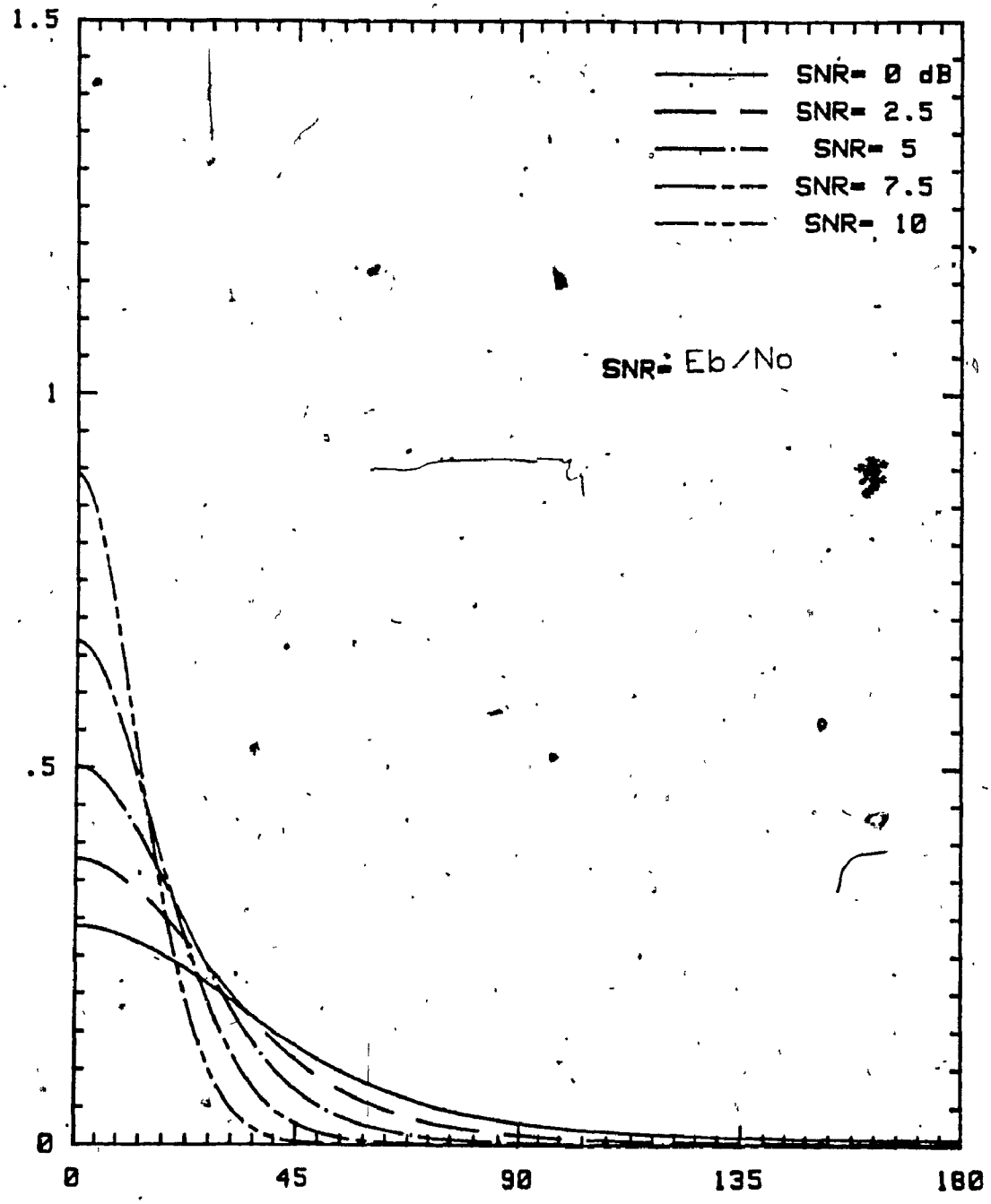

Figure 4.3 - Probability Density Function
Phase of the DPSK received vector

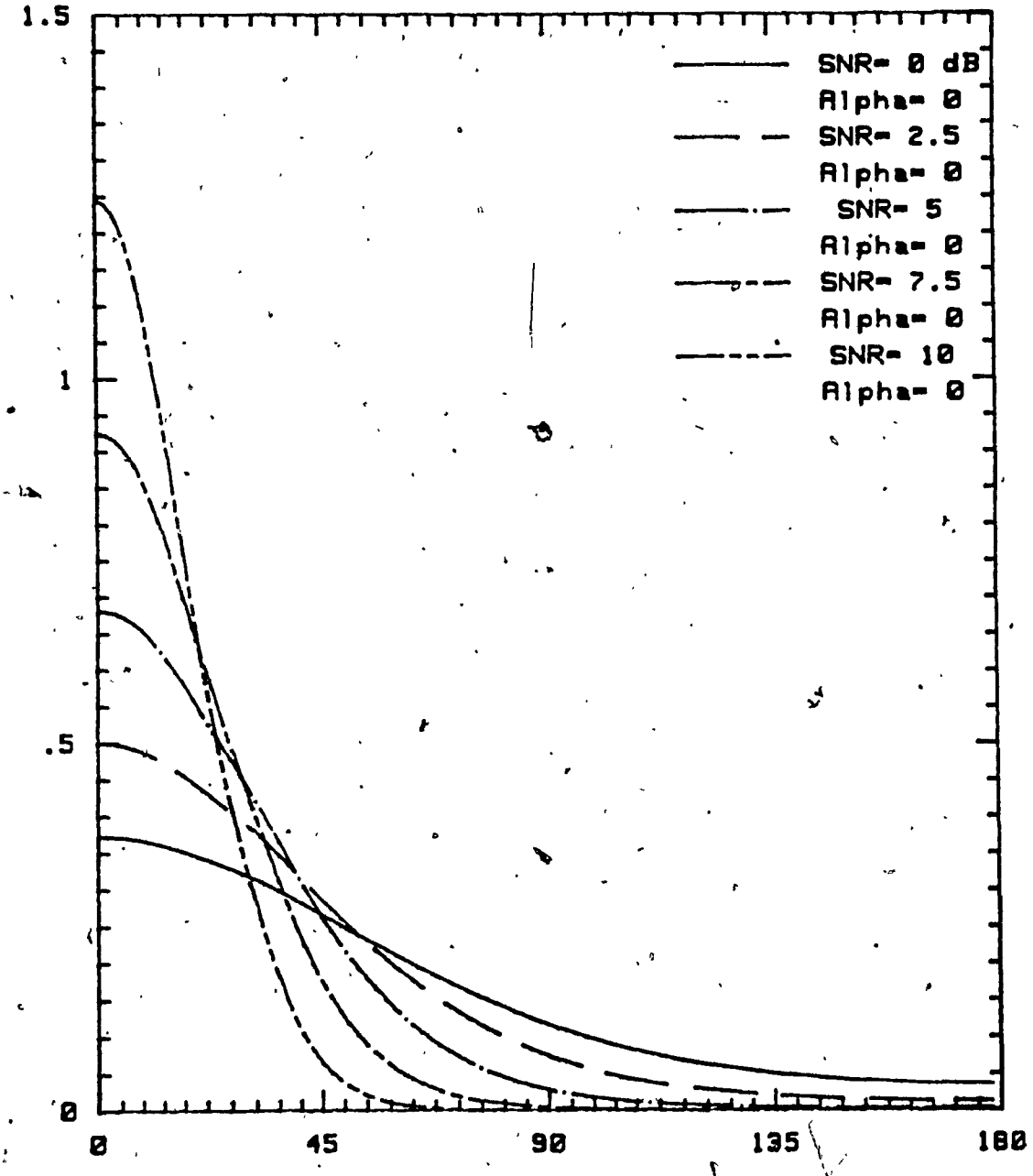

Figure 4.5 – Probability Density Function of the random variable at the output of the phase comparator

error will occur if and only if the noise vector η_2 exceeds the vector v.

$$Pr\,(error\,/\phi_1\,,\,\psi) = \int_{v}^{+\infty} f_{\eta_2}(x)\,dx \tag{4.29}$$

From Figure 4.2, we have

$$A\cos\phi_1 = v\cos\psi \tag{4.30}$$

and

$$v = A\frac{\cos\phi_1}{\cos\psi} \tag{4.31}$$

Equation (4.29) becomes

$$P_r\,(error\,/\phi_1\,,\,\psi) = \int_{A\frac{\cos\phi_1}{\cos\psi}}^{+\infty} f_{\eta_2}(x)\,dx \tag{4.32}$$

4.3 The probability density function of η_2

We have

$$\eta_2 = \sqrt{n_{c2}^2 + n_{s2}^2} \tag{4.33}$$

where n_{c2} and n_{s2} are additive white noise with power spectral density $N_0/2$. The joint probability density function is given by

$$f_{n_{c2},\,n_{s2}}(x\,,y) = \frac{1}{\pi N_0} e^{-(x^2 + y^2)/N_0} \tag{4.34}$$

let

$$n_{c\,2} = \eta_2 \cos\theta 2 \tag{4.35}$$

and

$$n_{s\,2} = \eta_2 \sin\theta_2 \tag{4.36}$$

We note that

$$dn_{c\,2}\,dn_{s\,2} = \eta_2 d\,\eta_2 d\,\theta_2 \tag{4.37}$$

and

$$f_{n_{c2},\,n_{s2}}(n_{c\,2},\,n_{s\,2}) = \eta_2 f_{\eta_2,\,\theta_2}(\eta_2,\,\theta_2) \tag{4.38}$$

Using equations (4.34) and (4.37), we have

$$f_{\eta_2,\,\theta_2}(\eta_2,\,\theta_2) = \frac{\eta_2}{\pi N_0} e^{-\frac{1}{N_0}\eta_2^2} \tag{4.39}$$

Integrating over all possible values of θ_2, we get the marginal density function of η_2

$$f_{\eta_2}(\eta_2) = \frac{2\eta_2}{N_0} e^{-\frac{\eta_2^2}{N_0}} \tag{4.40}$$

Combining equation (4.32) and equation (4.40) gives

$$Pr\,(error\,/\phi_1\,,\,\psi) = \int_{A\frac{\cos\phi_1}{\cos\psi}}^{+\infty} \frac{2\eta_2}{N_0} e^{-\frac{\eta_2^2}{N_0}} d\,\eta_2$$

$$= e^{-\frac{A^2}{N_0}\frac{\cos^2\phi_1}{\cos^2\psi}} \tag{4.41}$$

From figure (4.2), we notice that

$$\psi = 180 - \phi_1 - \theta_2 \tag{4.42}$$

The conditional probability of error defined in equation (4.30) becomes

$$Pr\,(error\,/\phi_1,\,\theta_2) = e^{-\frac{A^2}{N_0}\frac{\cos^2\phi_1}{\cos(\theta_2+\phi_1)}} \tag{4.43}$$

To find the probability of error given the angle ϕ_1, we have to average over all possible values of the angle θ_2 for which an error is made, i.e.

$$Pr\,(error\,/\phi_1) = \int_{-\pi}^{+\pi} e^{-\frac{A^2}{N_0}\frac{\cos^2\phi_1}{\cos^2(\theta_2+\phi_1)}} f_{\theta_2}(\theta_2) d\,\theta_2 \tag{4.44}$$

From Figure 4.2, we notice that it is possible to make an error if and only if the angle θ_2 is in the interval $[-\pi/2 - \phi_1\,,\,\pi/2 - \phi_1]$. Equation (4.44) becomes

$$Pr\,(error\,/\phi_1) = \int_{-\pi/2-\phi_1}^{\pi/2-\phi_1} e^{-\frac{A^2}{N_0}\frac{\cos^2\phi_1}{\cos^2(\phi_1+\theta_2)}} f_{\theta_2}(\theta_2) d\,\theta_2$$

$$= \int_{-\pi/2}^{+\pi/2} e^{-\frac{A^2}{N_0}\frac{\cos^2\phi_1}{\cos^2\theta}} f_{\theta_2}(\theta) d\,\theta \tag{4.45}$$

The probability density function $f_{\theta_2}(\theta)$ can be found from equation (4.39)

$$f_{\theta_2}(\theta) = \int_0^{+\infty} \frac{\eta_2}{\pi N_0} e^{-\frac{\eta_2}{N_0}} d\eta_2$$

$$= \frac{1}{2\pi} \tag{4.46}$$

θ_2 is uniformly distributed over that interval $[-\pi, +\pi]$.

Combining equations (4.45) and (4.46) gives

$$Pr(error/\phi_1) = \frac{1}{2\pi} e^{-\frac{A^2}{N_0}\cos^2\phi_1} \int_{-\pi/2}^{+\pi/2} e^{-\frac{A^2}{N_0}\cos^2\phi_1\tan^2\theta} d\theta \tag{4.47}$$

let

$$y = \int_{-\pi/2}^{+\pi/2} e^{-\frac{A^2}{N_0}\cos^2\phi_1\tan^2 x} dx \tag{4.48}$$

and

$$z = \tan(x) \tag{4.49}$$

$$dz = (1 + \tan^2 x)dx = (1 + z^2)dx \tag{4.50}$$

Changing these variables in equation (4.48), we get

$$y = \int_{-\infty}^{+\infty} \frac{1}{1+x^2} e^{-\frac{A^2}{N_0}x^2\cos^2\phi_1} dx \tag{4.51}$$

let us define b as

$$b = \frac{A^2}{N_0}\cos^2\phi_1 \tag{4.52}$$

equation (4.51) becomes

$$y = \int_{-\infty}^{+\infty} \frac{1}{1+x^2} e^{-bx^2} dx \tag{4.53}$$

Taking the derivative of y with respect to b gives

$$y' = \frac{dy}{db} = -\int_{-\infty}^{+\infty} \frac{x^2}{1+x^2} e^{-bx^2} dx \tag{4.54}$$

Substracting y' from y, we obtain the simple integral

$$y - y' = \int_{-\infty}^{+\infty} \frac{1}{1+x^2} e^{-bx^2} dx + \int_{-\infty}^{+\infty} \frac{x^2}{1+x^2} e^{-bx^2} dx$$

$$= \int_{-\infty}^{+\infty} e^{-bx^2} dx = \sqrt{\pi/b} \tag{4.55}$$

Hence

$$y - y' = \sqrt{\pi/b} \tag{4.56}$$

which is a linear differential equation.

We have

$$\frac{dy}{dx} - y + \sqrt{\pi/x} = 0 \tag{4.57}$$

where $x = \frac{A^2}{N_0}\cos^2\phi_1$. Using the Laplace transform, we get

$$sY(s) - y(0) - Y(s) + \frac{\pi}{\sqrt{s}} = 0 \tag{4.58}$$

$$(s-1)Y(s) + \frac{\pi}{\sqrt{s}} - \pi = 0 \tag{4.59}$$

Solving for $Y(s)$, we obtain

$$Y(s) = \frac{\pi}{s-1} - \frac{\pi}{\sqrt{s}\,(s-1)} \tag{4.60}$$

Taking the Laplace inverse of equation (4.60), we get [3]

$$\begin{aligned} y(x) &= \pi e^x - \pi e^x \, erf\,(\sqrt{x}) \\ &= \pi e^x \left[1 - erf\,(\sqrt{x})\right] \end{aligned} \tag{4.61}$$

But, $x = b$ and given by equation (4.52), equation (4.61) becomes

$$y = \pi e^{\frac{A^2}{N_0}\cos^2\phi_1}\left[1 - erf\,(\frac{A}{N_0}\cos\phi_1)\right] \tag{4.62}$$

Combining equations (4.47) and (4.62), the conditional probability of error will be given by the expression

$$P_r(error/\phi_1) = \frac{y}{2\pi} e^{-\frac{A^2}{N_0}\cos^2\phi_1}$$

$$= \frac{1}{2}\left[1 - erf\left(\frac{A}{N_0}\cos\phi_1\right)\right] \tag{4.63}$$

Averaging over all possible values of the the angle ϕ_1, the probability of bit error for the DPSK signal will be given by

$$P_e = \int_{-\pi}^{+\pi} P_r(error/\phi_1) f_{\phi_1}(\phi_1) d\phi_1$$

$$= \frac{1}{2} e^{-\frac{A^2}{N_0}} + \frac{A}{\sqrt{16\pi N_0}} \int_{-\pi}^{+\pi} \cos\phi_1 \, e^{-\frac{A^2}{N_0}\sin^2\phi_1} d\phi_1$$

$$- \frac{A}{\sqrt{16\pi N_0}} \int_{-\pi}^{+\pi} \cos\phi_1 \, e^{-\frac{A^2}{N_0}\sin^2\phi_1} erf^2\left(\frac{A}{N_0}\cos\phi_1\right) d\phi_1 \tag{4.64}$$

The two integrals in equation (4.64) are periodic functions of ϕ_1 with period 2π. They are symmetric and alternate each half period; that is, their functional dependence on ϕ_1 satisfies the condition

$$f(\phi_1 + \pi) = -f(\phi_1), \qquad \text{for } all \ \phi_1$$

The average value of any such function over one period is zero. Hence

$$\int_{-\pi}^{+\pi} \cos\phi_1 \, e^{-\frac{A^2}{N_0}\sin^2\phi_1} d\phi_1 = 0 \tag{4.65}$$

$$\int_{-\pi}^{+\pi} \cos\phi_1 \, e^{-\frac{A^2}{N_0}\sin^2\phi_1} \, erf^{\,2}\left(\frac{A}{\sqrt{N_0}}\cos\phi_1\right) d\phi_1 = 0 \qquad (4.66)$$

Using this fact, the average probability of bit error for the DPSK signal reduces to the well known expression

$$P_e = \frac{1}{2} e^{-\frac{A^2}{N_0}} \qquad (4.67)$$

The probability of error P_e is presented in Figure 4.6 as a function of signal-to-noise ratio. The next step is to investigate the effect of the low-pass filter on the performance of the system.

4.7 Effect of the LPF on the Performance of the System

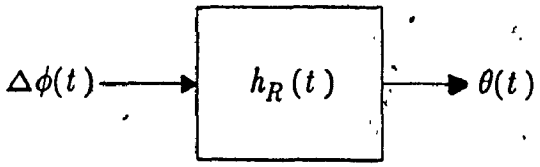

Figure 4.7 - Low pass filter

The output of a linear system is given by the convolution of the input signal with the impulse response of the system.

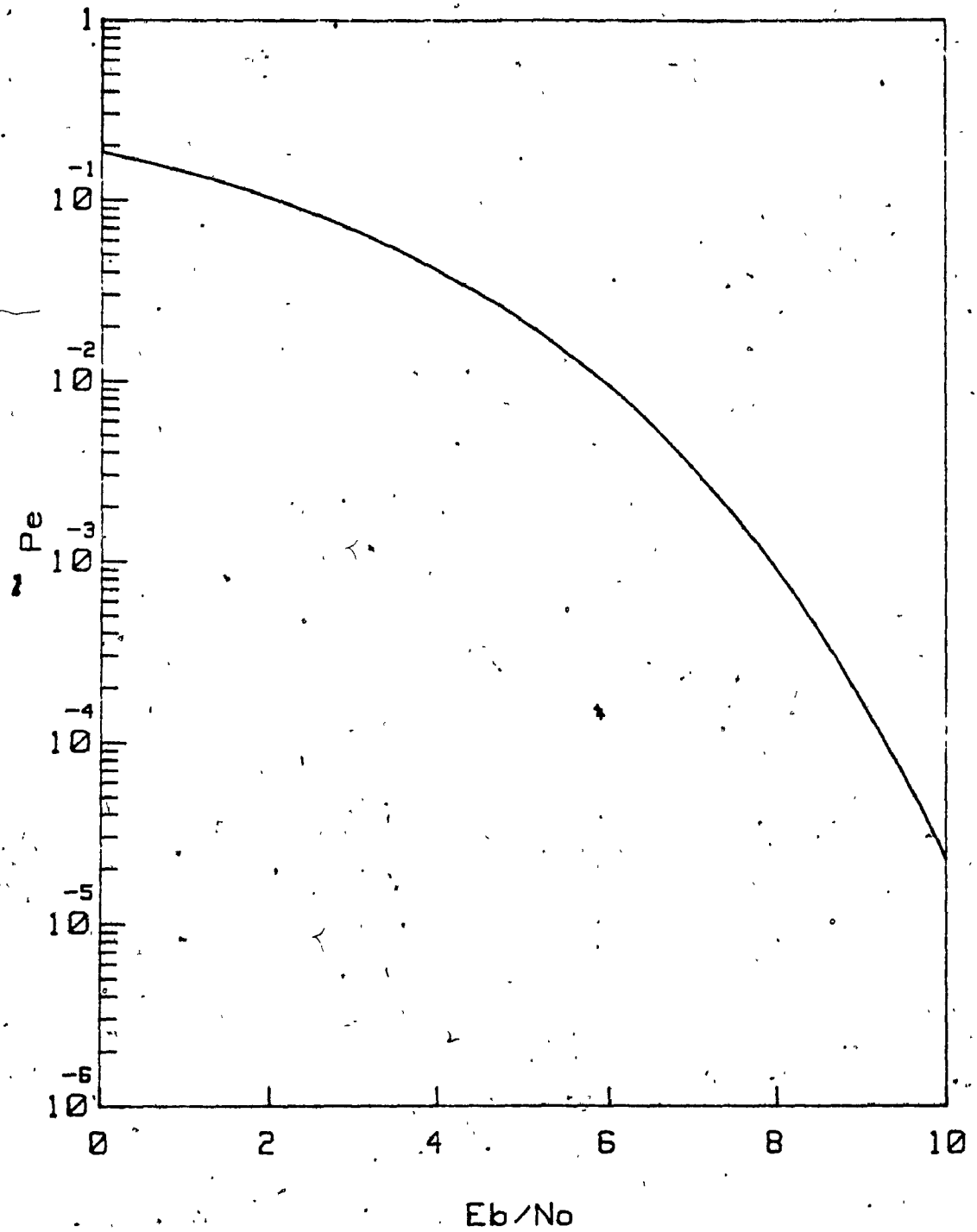

Fig. 4.6 - Average probability of error before the LPF

$$\theta(t) = \Delta\phi(t) * h_r(t)$$

$$= \int_{-\infty}^{+\infty} \Delta\phi(t-\tau) h_R(\tau) d\tau \tag{4.68}$$

where $*$ denotes the convolution, $\Delta\phi$ is a continuous random phase and $h_R(t)$ is the impulse response of the low-pass filter given by

$$h_r(t) = F^{-1}\left\{\sqrt{R(f,\alpha)}\right\} \tag{4.69}$$

Our concern in this section is to characterize the random process output of the low-pass filter when the input is a random process. It is well known that, when the input is a Gaussian process the output is also a Gaussian process. However for a non-Gaussian input, the characteristics of the output process are not easily determined.

Given the autocorrelation function of the input process and the impulse response of the system, the autocorrelation function of the output process can be easily found. However, in order to find the probability of error, it is required to obtain the probability density function of the output process. The probability density function is not, in general, determined by the autocorrelation function or the mean of the output.

The following presents a method [21,23] to approximate the probability density function of the output filter based on numerical calculations.

Consider the output process $\theta(t)$ given by the equation (4.68), since $\theta(t)$ is a continuous random phase, it can be written in the form

$$\theta(t) = \int_{-\infty}^{+\infty} \Delta\phi(t-\tau)h_R(\tau)d\tau$$

$$\approx \lim_{\Delta\tau\to 0} \Delta\tau \sum_{n=-\infty}^{+\infty} \Delta\phi(t - n\Delta\tau)h_R(n\Delta\tau) \tag{4.70}$$

Writing the characteristic function of $\theta(t)$, we get

$$\Phi_\theta(\omega) = E(e^{j\omega\theta(t)})$$

$$= E\left[e^{j\omega\Delta\tau \sum_{n=-\infty}^{+\infty} \Delta\phi(t - n\Delta\tau)h_R(n\Delta\tau)}\right] \tag{4.71}$$

The random process $\Delta\phi(t - n\Delta\tau)$, $\Delta\phi(t - k\Delta\tau)$ with $n \neq k$ are assumed to be statistically independent [25]. The characteristic function in equation (4.71) becomes the product of an infinite number of independent characteristic functions.

$$\Phi_\theta(\omega) = \prod_{n=-\infty}^{+\infty} E\left[e^{j\omega\Delta\tau\Delta\phi(t - n\Delta\tau)h_R(n\Delta\tau)}\right] \tag{4.72}$$

But, we know that

$$E\left[e^{j\omega\Delta\tau\Delta\phi(t - n\Delta\tau)h_R(n\Delta\tau)}\right] = \Phi_{\Delta\Phi}\left(\omega\Delta\tau h_R(n\Delta\tau)\right) \tag{4.73}$$

Combining the two equations, we get

$$\Phi_\Theta(\omega) = \prod_{n=-\infty}^{+\infty} \Phi_{\Delta\Phi}\left(\omega\Delta\tau h_R(n\Delta\tau)\right) \tag{4.74}$$

where $\Phi_{\Delta\Phi}(\omega)$ is the characteristic function of the input random process. For a given $\Delta\tau$ and $h_R(t)$, $\Phi_{\Delta\Phi}(\omega)$ can be evaluated. The calculation of the characteristic function $\Phi_\Theta(\omega)$ is therefore possible.

The probability density function of the output process is then

$$f_\Theta(\theta) = \frac{1}{2\pi} \int_{-\infty}^{+\infty} \Phi_\Theta(\omega) e^{-j\omega\theta} d\omega$$

$$= \frac{1}{2\pi} \int_{\infty}^{+\infty} \prod_{=-\infty}^{+\infty} \Phi_{\Delta\Phi}\left(\omega\Delta\tau h_R(n\Delta\tau)\right) e^{-j\omega\theta} d\omega \qquad (4.75)$$

Since the input process is defined in the interval $[-\pi, \pi]$, it is quite logic that the output process will be also defined in the same interval modulo 2π.

We have

$$\Delta\Phi = \Phi_2 - \Phi_1 \qquad (4.76)$$

where Φ_1, Φ_2 are i.i.d random variables with probability density function given by equation (4.24)

$$f_{\Phi_1}(\theta) = \frac{1}{2\pi} e^{-\frac{A^2}{N_0}} + \frac{A}{\sqrt{4\pi N_0}} \cos\theta\, e^{-\frac{A^2}{N_0}\sin^2\theta} \left[1 + erf\left(\frac{A}{\sqrt{N_0}}\cos\theta\right)\right] \qquad (4.77)$$

Since $f_{\Phi_1}(\theta)$ is an even and periodic function of θ, its characteristic function $\Phi_{\Delta\Phi}(\omega)$ is a real and discrete function of ω.

$$\Phi_{\Phi_1}(\omega) = \int_{-\infty}^{+\infty} f_{\Phi_1}(\theta) e^{j\omega\theta} d\theta$$

$$= \sum_{n=-\infty}^{+\infty} \int_{-(n+1)\pi}^{-(n-1)\pi} f_{\Phi_1}(\theta) e^{j\omega\theta} d\theta \tag{4.78}$$

Changing θ by $\theta + n\pi$ and using the periodicity of $f_{\Phi_1}(\theta)$, we get

$$\Phi_{\Phi_1}(\omega) = \sum_{n=-\infty}^{+\infty} e^{j2\omega n\pi} \int_{-\pi}^{+\pi} f_{\Phi_1}(\theta) \cos(\omega\theta) d\theta \tag{4.79}$$

Note that

$$\sum_{n=-\infty}^{+\infty} e^{j2\omega n\pi} = \sum_{n=-\infty}^{+\infty} \delta(\omega - n) \tag{4.80}$$

and if we define c_n as

$$c_n = \int_{-\pi}^{+\pi} f_{\Phi_1}(\theta) \cos(n\theta) d\theta \tag{4.81}$$

$\Phi_{\Phi_1}(\omega)$ becomes

$$\Phi_{\Phi_1}(\omega) = \sum_{n=-\infty}^{+\infty} c_n \delta(\omega - n) \tag{4.82}$$

Since $\Delta\Phi = \Phi_2 - \Phi_1$, the characteristic function of $\Delta\Phi$ can be written as

$$\Phi_{\Delta\Phi}(\omega) = \Phi_{\Phi_1}{}^2(\omega)$$

$$= \sum_{n=-\infty}^{+\infty} c_n{}^2 \delta(\omega - n) \tag{4.83}$$

and the expression of $f_{\Delta\Phi}(\theta)$ becomes

$$f_{\Delta\Phi}(\theta) = \frac{1}{2\pi} + 2\sum_{n=1}^{+\infty} c_n{}^2 \cos(n\theta) \tag{4.84}$$

At high signal-to-noise ratio

for $\left|\frac{n_s}{A + n_c}\right| \ll 1$ (e.g. $10\log_{10}(\frac{A^2}{n_s{}^2}) > 5dB$),

$$\phi_i = \tan^{-1}\left(\frac{n_{si}}{A + n_{ci}}\right) \approx \frac{n_{si}}{A} \quad in\ rad \tag{4.85}$$

$$i = 1,2$$

ϕ_i can be treated as a Gaussian variable with zero mean and variance $N_0/2A^2$. So that its probability density function can be written as

$$f_{\Phi_i}(x) = \frac{A}{\pi N_0} e^{-x^2 \frac{A^2}{N_0}} \tag{4.86}$$

Since ϕ_1, ϕ_2 are i.i.d random variables, the characteristic function of Ψ is given by

$$\Phi_{\Delta\Phi}(\omega) = E\left(e^{j\omega(\phi_1 - \phi_2)}\right) = E\left(e^{j\omega\phi_1}\right) E\left(e^{-j\omega\phi_2}\right)$$

$$= \Phi_{\Phi_1}(\omega)\Phi_{\Phi_2}{}^{*}(\omega) \tag{4.87}$$

But $\Phi_{\Phi_1}(\omega)$ is given by

$$\Phi_{\Phi_1}(\omega) = e^{-\omega^2 N_0/4A^2} \tag{4.88}$$

so that $\Phi_{\Delta\Phi}(\omega)$ becomes

$$\Phi_{\Delta\Phi}(\omega) = e^{-\omega^2 N_0/2A^2} \tag{4.89}$$

Hence, $\Delta\Phi$ is a Gaussian process with zero mean and variance N_0/A^2.

The output of the detection filter, $\theta(t)$, is also a Gaussian process with variance

$$\sigma_\Theta{}^2 = \frac{N_0}{A^2} \int_{-\infty}^{+\infty} |H_R(f)|^2 df \tag{4.90}$$

But $H_R(f)$ is given by

$$H_R(f) = \sqrt{R(f, \alpha)} \tag{4.91}$$

Hence

$$\int_{-\infty}^{+\infty} |H_R(f)|^2 df = \int_{-\infty}^{+\infty} R(f, \alpha) df = 1$$

so that the variance of the output process becomes

$$\sigma_\Theta^2 = \frac{N_0}{A^2} \tag{4.92}$$

Based on the decision rule given by equation (4.11), the probability of bit error at the output of the low pass filter will be given by

$$P_{eo} = 1 - \frac{1}{\sigma_\Theta\sqrt{2\pi}} \int_{-\pi/2}^{+\pi/2} e^{-x^2/2\sigma_\Theta^2}\, dx$$

$$= 1 - erf\left(\frac{\pi}{2\sqrt{2}\sigma_\Theta}\right) \tag{4.93}$$

Repacing σ_Θ by its value, we get

$$P_{eo} = 1 - erf\left(\frac{A\,\pi}{\sqrt{8N_0}}\right) \tag{4.94}$$

with $E_b = A^2$, P_{eo} becomes

$$P_{eo} = erfc\left(\sqrt{\frac{\pi^2}{8}\frac{E_b}{N_0}}\right) \tag{4.95}$$

P_{eo} is shown in the next figure. We notice that the probability of error is improved by the low-pass filter.

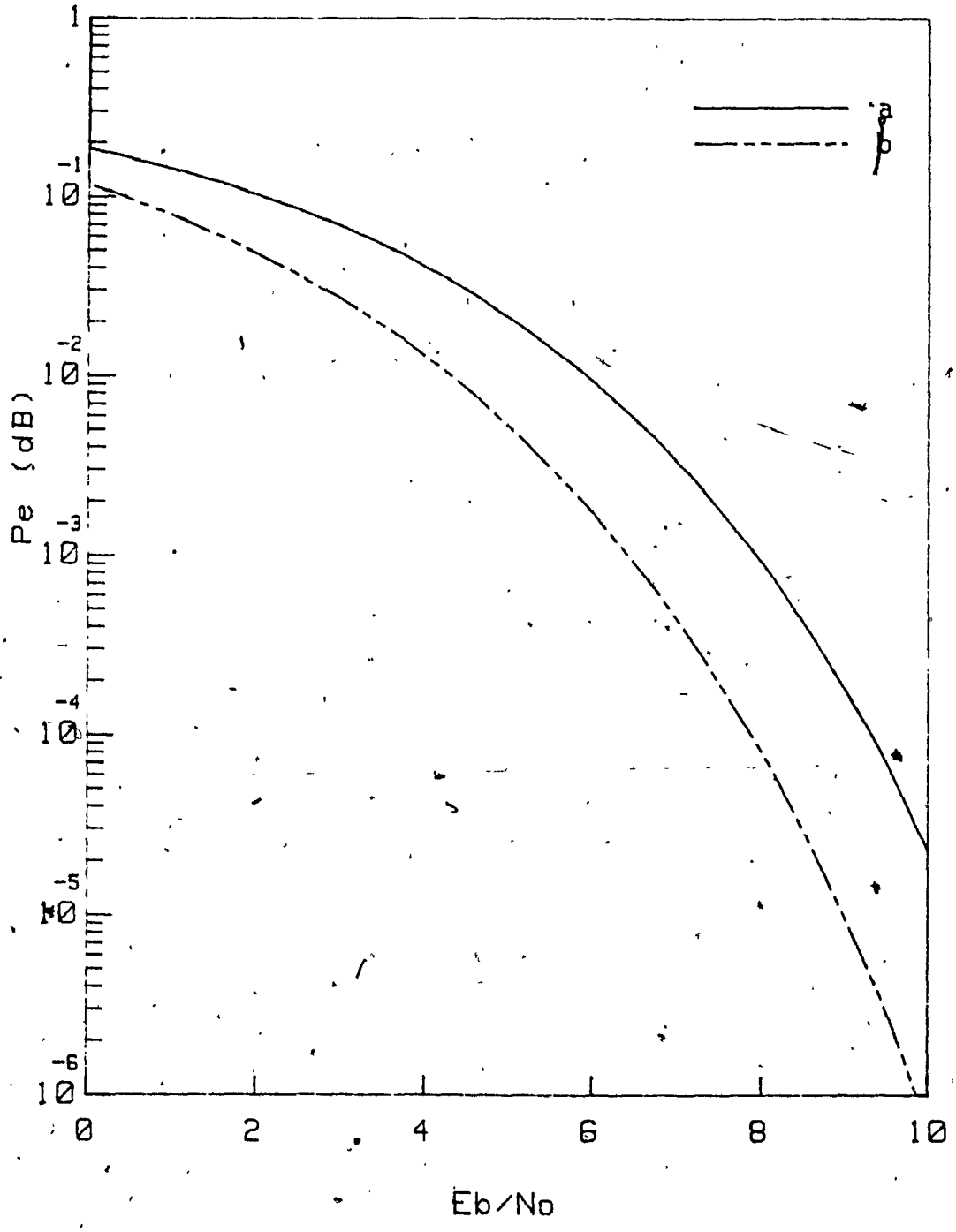

Fig. 4.7 - Average probability of error

a - before the LPF, b - after the LPF

CHAPTER FIVE

CONCLUSIONS AND SUGGESTIONS FOR FURTHER RESEARCH

5.1 Conclusions

A bandwidth-efficient constant-envelope differential PSK modulation/demodulation schemes for TDMA applications was presented and studied. Both spectral properties and performance were analyzed.

Since phase modulation is a nonlinear process, the spectrum of the base-band signal can not be used directly to predict that of the modulated signal. Rather the spectrum of the modulated signal was analyzed using the autocorrelation techniques. It has been shown that the bandwidth can be improved with narrow shaping low-pass filter. In fact, by varying the roll-off factor α of the Nyquist filter, the spectrum main-lobe remained almost the same but very low side-lobes were obtained.

The spectrum was computed using truncated shaping functions (of duration KT_b). It has been shown that for $K = 5$, the power spectral density was good enough to represent the case of the shaping low-pass filter having the impulse response with infinite time duration. The DPSK signal was compared to Offset QPSK and MSK signals. Although Offset QPSK and MSK belong to quadrature modulation family, the binary differential PSK offers almost the main-lobe and a lower high-order side-lobes than these signals which gives a promissing future for high-level DPSK signals.

The bit error performance of bandwidth efficient DPSK in linear channels was studied. After the linear phase comparator, it was shown that the probability of error is given by the well known expression $\frac{1}{2}e^{-\frac{A^2}{N_0}}$. At $P_e \leq 10^{-4}$, the power requirement of DPSK is approximatly 1 dB more than coherent PSK. Effects of the low pass filter at the receive end was discussed. The probability density function was computed, it has been shown that the performance at the output of the low-pass filter is independent of the roll-off factor α and is comparable to the coherent PSK.

5.2 Suggestions for Further Research

The study of the the introduced binary DPSK modulation/demodulation scheme can be extended to the M-ary DPSK cases. Some suggestions for further research are.

* *M-ary Differential PSK:* Only binary DPSK was considered throughout our studies. With M-ary DPSK, we can improve the bandwidth efficiency. These signals can offer a good trade-off between power and bandwidth. We believe that the study of multi-level DPSK modulation/demodulation and specially DQPSK will be desirable for TDMA applications.

* *Implementation of M-ary Differential PSK using Digital Signal Processors:* Digital spectral analysis has been given a tremendous boost by the introduction of the fast Fourier transform (FFT). These computationally efficient algorithms have gained widespread use in many diverse scientific disciplines, making possible accuracies and resolutions that could not even be contemplated before with an analog approach. Many state-of-the-art digital signal

processors (DSP) are now available and can be used to implement M-ary DPSK with sufficiently high speed to permit real time processing for low-capacity modems as mobile communications or VSAT (Very small Aperture Terminal) applications. DSP based implementation of modems is attractive because adaptive algorithms and flexible bit rate or modem configurations can be realized.

REFERENCES

[1] K. Hirade et al., "Error rate performance of digital FM with differential detection in land mobile radio channels," *IEEE Trans. Veh. Technol.*, vol. VT. 28, pp. 204-212, Aug, 1979.

[2] T. Le-Ngoc, "A serial demodulation technique for differential offset QPSK," *IEEE Montech '86,* pp. 243-245, Sept. 29-Oct. 1, 1986.

[3] S. Elnoubi, "Analysis of GMSK with differential detection in land mobile radio channels," *IEEE Trans. Veh. Technol.*, vol. VT. 35, pp. 162-167, Nov., 1986.

[4] F. Amoroso, "The bandwidth of digital data signals," *IEEE Trans. Mag.*, vol. 18, pp. 13-24, Nov., 1980.

[5] L. J. Greenstein, "Spectra of PSK signals with overlapping baseband pulses," *IEEE Trans. Commun.*, vol. COM. 25, pp. 523-530, May, 1977.

[6] C. E. Sundberg, "Continuous phase modulation," *IEEE Trans. Commun. Mag.*, vol. 24, pp. 25-38, April, 1986.

[7] G. J. Garrison, "A power spectral density analysis for digital FM," *IEEE Trans. Commun.*, vol. 23, pp. 1228-1243, Nov., 1975.

[8] R. F. Pawula, "On the theory of error rates for narrow-band digital FM," *IEEE Trans. Commun.*, vol. COM. 29, pp. 1634-1643.

[9] J. E. Mazo and J. Salz, "Theory of error rates for digital FM," *Bell Syst. Tech. J.*, vol. xx, pp. 1511-1535, June, 1966

[10] J. G. Smith, "Spectrally efficient modulation," *in Proc. IEEE Int. Conf. Commun.* (ICC' 77), pp. 3.1-37/3.1-41, June, 1977.

[11] A. P. Clark, "Digital modems for land mobile radio," *IEEE Proc.*, vol. 132,

pp. 348-362, Aug., 1985.

[12] T. Le.Ngoc, "A differential offset-QPSK modulation/demodulation technique for point-to-multipoint radio systems," , *Globecom '87*, Tokyo Japan, Nov. 15-18, 1987.

[13] P. K. M. Ho and P. J. Mclane, "Power spectral density of digital continuous phase modulation with correlated data symbols. Part 1: Autocorrelation function method," *IEE Proc.*, vol. 133, pp. 95-105, Febr., 1986.

[14] P. K. M. Ho and P. J. Mclane, "Power spectral density of digital continuous phase modulation with correlated data symbols. Part 2: Rowe-Prabhu method," *IEE Proc.*, vol. 133, pp. 106-114, Febr., 1986.

[15] T. Le-Ngoc, "A serial demodulation technique for differential offset QPSK," *Montech '86*, Montreal, Sept. 29-Oct. 3, 1986.

[16] C. R. Cahn, "Performance of digital phase-modulation communication systems," *IRE Trans. Commun. Syst.*, vol. 42, pp. 142-145, May, 1959.

[17] F. Amoroso, "The use of quasi-bandlimited pulses in MSK transmission," *IEEE Trans. Commun.*, vol COM-27, pp. 1616-1624, Oct., 1979.

[18] V. I. Krylov, *Approximate Calculation of Integrals*, A. H. Strond, New York: Macmillan, 1962.

[19] I. Korn, *Digital Communication*, Van Nostran Reinhold, 1985.

[20] G. Fodor, *Laplace Transform in Engineering*, Budapest, 1965.

[21] W. B. Davenport, Jr, and W. L. Roots, *An Introduction to the Theory of Random Signals and Noise*, McGraw Hill, 1958.

[22] S. Haykin, *Communication Systems*, Second Edition, John Wiley & Sons, 1983.

[23] A. Papoulis, *Probability, Random Variables, and Stochastic Processes*,

McGraw Hill, 1984.

[24] K. J. P. Fonseka and N. Ekanayake, "Differential detection of narrow-band binary FM," *IEEE Trans. Commun.*, vol. COM-33, pp. 725-729, July 1985.

[25] R. E. Ziemer and W. H. Tranter, *Principles of Communications,* Houghton Milfin, 1976.

[26] R.F. Pawula et al., "Distribution of the phase angle between two vectors perturbed by Gausslan noise," *IEEE trans. Commun.*, vol. COM. 30, pp. 1828-1841, Aug., 1982

APPENDIX A

FOURIER INVERSE OF THE SQUARE ROOT OT NYQUIST PULSE

We have

$$\sqrt{R(f\ ,\alpha)} = \begin{cases} \sqrt{T_b} & 0 \le |f\ | \le (1+\alpha) f_0 \\ \sqrt{T_b}\cos\left[\frac{\pi}{4\alpha f_0}(|f\ | - (1-\alpha)f_0\right] & (1-\alpha)f_0 \le |f\ | \le (1+\alpha)f_0 \\ 0. & \textit{elsewhere} \end{cases}$$

(A.1)

Since $\sqrt{R(f\ ,\alpha)}$ is an even function, its inverse Fourier transform is a real function of time t and given by

$$r(t\ ,\alpha) = 2\int_0^{+\infty} \sqrt{R(f\ ,\alpha)}\cos(2\pi f t)df \qquad (A.2)$$

Replacing $\sqrt{R(f\ ,\alpha)}$ by its expression, we get

$$R(t\ ,\alpha) = 2\sqrt{T_b}\int_0^{(1-\alpha)f_0} \cos(2\pi f t)df$$

$$+ 2\sqrt{T_b}\int_{(1-\alpha)f_0}^{(1+\alpha)f_0} \cos\left[\frac{\pi}{4\alpha f_0}(f\ - (1-\alpha)f_0)\right]\cos(2\pi f t)df$$

(A.3)

Changing f by $(f - f_0)$ gives

$$r(t\ ,\alpha) = \frac{T_b}{\pi t}\sin\left(2\pi f_0 t\,(1-\alpha)\right)$$

$$+ 2T_b \int_{-\alpha f_0}^{\alpha f_0} \cos\left(\frac{\pi}{4\alpha f_0}(f - \alpha f_0)\right)\cos(2\pi t\,(f + f_0))df \qquad \text{(A.4)}$$

Solving the integral and letting $x = 2f_0 t$, we get

$$r(t\ ,\alpha) = \frac{2\sqrt{T_b}\,f_0}{\pi x}\sin(\pi(1-\alpha)x) + \frac{8\alpha f_0\sqrt{T_b}}{\pi\left(1-(4\alpha x)^2\right)}\cos(\pi(1+\alpha)x)$$

$$+ \frac{32\alpha f_0 T_b\, x}{\pi\left(1-(4\alpha x)^2\right)}\sin(\pi(1-\alpha)x) \qquad \text{(A.5)}$$

and rearranging terms

$$r(t\ ,\alpha) = \frac{\sin\left(\pi(1-\alpha)x\right)}{\pi x\sqrt{T_b}}$$

$$= \frac{4\alpha}{\pi\sqrt{T_b}\left(1-(4\alpha x)^2\right)}\left[\cos\left((1+\alpha)\pi x\right) + 4x\sin\left((1-\alpha)\pi x\right)\right]$$

(A.6)

APPENDIX B

VERIFICATION OF EQUATION (4.74) IN THE CASE OF GAUSSIAN INPUT

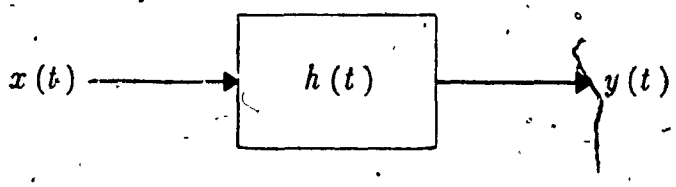

Figure B.1 - Linear system.

The output process y(t) is related to the input signal by

$$y(t) = \int_{-\infty}^{+\infty} x(t-\tau)h(\tau)d\tau \tag{B.1}$$

where x(t) is a zero-mean Gaussian process with power spectrum*

$$S_x(f) \triangleq \frac{N_0}{2}, \qquad -\infty < f < \infty \tag{B.2}$$

The characteristic function of the output process y(t) can be written as

* The dimension of N_0 are Watts per cycle per second, or joules. We shall always define the power spectra on a bilateral frequency basis, $-\infty < f < \infty$.

$$\Phi_Y(\omega) = \prod_{n=-\infty}^{+\infty} \Phi_X\left(\omega \Delta\tau h(n\,\Delta\tau)\right) \tag{B.3}$$

But, the characteristic function of a zero-mean Gaussian process is given by [23]

$$\Phi_X(\omega) = e^{-N_0\omega^2/4} \tag{B.4}$$

Combining equation (B.3) and (B.4), $\Phi_Y(\omega)$ becomes

$$\Phi_Y(\omega) = \prod_{n=-\infty}^{+\infty} e^{-\frac{N_0}{4}\left(\omega\Delta\tau h(n\,\Delta\tau)\right)^2}$$

$$= \exp\left[-\frac{N_0}{4}\omega^2 \sum_{n=-\infty}^{+\infty} h^2(n\,\Delta\tau)(\Delta\tau)^2\right] \tag{B.5}$$

The summation in equation (B.5) can be written in the equivalent form [25],

$$\sum_{n=-\infty}^{+\infty} h^2(n\,\Delta\tau)(\Delta\tau)^2 \overset{\Delta}{=} \sum_{n=-\infty}^{+\infty} h(n\,\Delta\alpha)h(n\,\Delta\beta)\Delta\alpha\Delta\beta$$

$$= \sum_{n=-\infty}^{+\infty}\sum_{n=-\infty}^{+\infty} h(n\,\Delta\alpha)h(i\,\Delta\beta)\delta(n\,\Delta\alpha - i\,\Delta\beta)\Delta\alpha\Delta\beta \tag{B.6}$$

Taking the limit when $\Delta\alpha \to 0$ and $\Delta\beta \to 0$, we get

$$\lim_{\Delta\tau \to 0} \sum_{n=-\infty}^{+\infty} h^2(n\,\Delta\tau)(\Delta\tau)^2 = \int_{-\infty}^{+\infty} \int_{-\infty}^{+\infty} h(\alpha)h(\beta)\delta(\alpha-\beta)d\alpha d\beta$$

$$= \int_{-\infty}^{+\infty} h^2(\alpha)d\alpha \qquad \text{(B.7)}$$

Using the well-known Parseval equation from the Fourier theory,

$$\int_{-\infty}^{+\infty} h^2(\alpha)d\alpha = \int_{-\infty}^{+\infty} |H(f)|^2 df \qquad \text{(B.8)}$$

where H(f) is the the Fourier transform of $h(\alpha)$. Equation (4.64) is nothing else than the bandwidth B_w of the system, hence the characteristic function $\Phi_Y(\omega)$ becomes the result that we all know

$$\Phi_Y(\omega) = e^{-\frac{N_0}{4}B_w\omega^2} \qquad \text{(B.9)}$$

Hence the output process is also additive with power spectral density $N_0B_w/2$.

APPENDIX C

POWER SPECTRAL DENSITY COMPUTATION

The PSD to compute is given by the expression

$$S(f) = \sum_{i=1}^{K} \left(S_{b,0}(f) - S_{b,K}(f) \right)$$

$$= 2Re \left[\sum_{i=1}^{K-1} \left(S_{b,i}(f) - S_{b,K}(f) \right) e^{-j2\pi f i T_b} \right]$$

where KT_b is the duration of the shaping function and the function $S_{b,i}(f)$ is given by

$$S_{b,i}(f) = \sum_{n=1}^{2^{K-i}} Z_n(f) Z_{2^i n-1}{}^*(f)$$

$Z_i(f)$ is the Fourier transform of the function $z_i(t)$, $z_i(t)$ follows the form

$$z_1(t) = \cos\left(\frac{\pi}{2} h_0(t)\right) \cos\left(\frac{\pi}{2} h_1(t)\right) \cdots \cos\left(\frac{\pi}{2} h_K(t)\right)$$

$$z_2(t) = \cos\left(\frac{\pi}{2} h_0(t)\right) \cos\left(\frac{\pi}{2} h_1(t)\right) \cdots \sin\left(\frac{\pi}{2} h_K(t)\right)$$

$$z_{\frac{2^K}{2}}(t) = \cos\left(\frac{\pi}{2} h_0(t)\right) \sin\left(\frac{\pi}{2} h_1(t)\right) \cdots \sin\left(\frac{\pi}{2} h_K(t)\right)$$

The quality of this microfiche is heavily dependent upon the quality of the thesis submitted for microfilming.

Please refer to the National Library of Canada target (sheet 1, frame 2) entitled:

CANADIAN THESES

NOTICE

La qualité de cette microfiche dépend grandement de la qualité de la thèse soumise au microfilmage.

Veuillez consulter la cible de la Bibliothèque nationale du Canada (microfiche 1, image 2) intitulée:

THÈSES CANADIENNES

AVIS

$$z_{2^K}(t) = \sin\left(\frac{\pi}{2}h_0(t)\right)\sin\left(\frac{\pi}{2}h_1(t)\right)\cdots\sin\left(\frac{\pi}{2}h_K(t)\right)$$

with

$$h_i(t) = h_l\left(t - \left(\frac{K}{2} - i\right)T_b\right) \qquad 0 \le |t| \le \frac{T_b}{2}$$

```
!  ************************************************
!          Power Spectral Density Fumction
!            Wave shape of duration 5Tb
!  ************************************************
Vx=0
Space=-.3
DEG
curve:
LINE TYPE 1
INPUT "WHAT IS THE DURATION OF THE WAVE SHAPE",Sd1
INPUT "WHAT IS THE VALUE OF ACCURACY N",N
DIM W1(600),W2(600),W3(600),W4(600),W5(600)
DIM Z2(600),Z3(600),Z4(600),Z5(600),Z6(600),Z7(600)
DIM Z8(600),Z9(600),Z10(600),Z11(600),Z12(600)
DIM Z13(600),Z14(600),Z15(600),Z16(600),Z17(600)
DIM Z18(600),Z19(600),Z20(600),Z21(600),Z22(600)
DIM Z23(600),Z24(600),Z25(600),Z26(600),Z27(600)
DIM Z28(600),Z29(600),Z30(600),Z31(600),Z32(600)
DIM Punct(150),Xs(150),Tm1(600),F1(600),F2(600)
FOR R=0 TO 1 STEP .5
Ts=20/N
Fs=1/20
Kp=90
M=0
J=0
V=1
B1=1
B0=1
B5=1
S7=1-R+4*R/PI
FOR K=-2.5 TO 2.5+Ts/4 STEP Ts
S1=1-(4*R*K)^2
K1=180*K*(1-R)
```

```
IF ABS(S1)<5.E-10 THEN S1=0
IF K=0 THEN
S5=1-R+4*R/PI
ELSE
IF R=0 THEN
S5=SIN(180*K)/(PI*K)
ELSE
IF S1=0 THEN
S5=R*COS(45*(1-1/R))-2*R*SIN(45*(1-1/R))/PI
ELSE
S5=(SIN(K1)/K+4*R*(COS(180*K*(1+R))+4*R*K*SIN(K1))/S1)/PI
END IF
END IF
END IF
S5=S5/S7
IF ABS(K)<Sd1/2 THEN S5=0
IF ABS(S5)<5.E-10 THEN S5=0
S5=Kp*S5
PRINT S5,K
IF K<=-1.5+Ts/8 THEN
J=J+1
W1(J)=S5
Tm1(J)=K+2
ELSE
IF K<=-.5+Ts/8 THEN
W2(1)=W1(J)
V=V+1
W2(V)=S5
ELSE
IF K<=.5+Ts/8 THEN
W3(1)=W2(V)
B1=B1+1
W3(B1)=S5
ELSE
IF K<=1.5+Ts/8 THEN
W4(1)=W3(B1)
B0=B0+1
W4(B0)=S5
ELSE
W5(1)=W4(B0)
B5=B5+1
W5(B5)=S5
END IF
END IF
END IF
END IF
NEXT K
!  ************************************************************
!  ********************* PSD Cmoputation **********************
!  ************************************************************
FOR I=1 TO J-1
```

```
Z2(I)=COS(W1(I))*COS(W2(I))*COS(W3(I))*COS(W4(I))*SIN(W5(I))
Z3(I)=COS(W1(I))*COS(W2(I))*COS(W3(I))*SIN(W4(I))*COS(W5(I))
Z4(I)=COS(W1(I))*COS(W2(I))*COS(W3(I))*SIN(W4(I))*SIN(W5(I))
Z5(I)=COS(W1(I))*COS(W2(I))*SIN(W3(I))*COS(W4(I))*COS(W5(I))
Z6(I)=COS(W1(I))*COS(W2(I))*SIN(W3(I))*COS(W4(I))*SIN(W5(I))
Z7(I)=COS(W1(I))*COS(W2(I))*SIN(W3(I))*SIN(W4(I))*COS(W5(I))
Z8(I)=COS(W1(I))*COS(W2(I))*SIN(W3(I))*SIN(W4(I))*SIN(W5(I))
Z9(I)=COS(W1(I))*SIN(W2(I))*COS(W3(I))*COS(W4(I))*COS(W5(I))
Z10(I)=COS(W1(I))*SIN(W2(I))*COS(W3(I))*COS(W4(I))*SIN(W5(I))
Z11(I)=COS(W1(I))*SIN(W2(I))*COS(W3(I))*SIN(W4(I))*COS(W5(I))
Z12(I)=COS(W1(I))*SIN(W2(I))*COS(W3(I))*SIN(W4(I))*SIN(W5(I))
Z13(I)=COS(W1(I))*SIN(W2(I))*SIN(W3(I))*COS(W4(I))*COS(W5(I))
Z14(I)=COS(W1(I))*SIN(W2(I))*SIN(W3(I))*COS(W4(I))*SIN(W5(I))
Z15(I)=COS(W1(I))*SIN(W2(I))*SIN(W3(I))*SIN(W4(I))*COS(W5(I))
Z16(I)=COS(W1(I))*SIN(W2(I))*SIN(W3(I))*SIN(W4(I))*SIN(W5(I))
Z17(I)=SIN(W1(I))*COS(W2(I))*COS(W3(I))*COS(W4(I))*COS(W5(I))
Z18(I)=SIN(W1(I))*COS(W2(I))*COS(W3(I))*COS(W4(I))*SIN(W5(I))
Z19(I)=SIN(W1(I))*COS(W2(I))*COS(W3(I))*SIN(W4(I))*COS(W5(I))
Z20(I)=SIN(W1(I))*COS(W2(I))*COS(W3(I))*SIN(W4(I))*SIN(W5(I))
Z21(I)=SIN(W1(I))*COS(W2(I))*SIN(W3(I))*COS(W4(I))*COS(W5(I))
Z22(I)=SIN(W1(I))*COS(W2(I))*SIN(W3(I))*COS(W4(I))*SIN(W5(I))
Z23(I)=SIN(W1(I))*COS(W2(I))*SIN(W3(I))*SIN(W4(I))*COS(W5(I))
Z24(I)=SIN(W1(I))*COS(W2(I))*SIN(W3(I))*SIN(W4(I))*SIN(W5(I))
Z25(I)=SIN(W1(I))*SIN(W2(I))*COS(W3(I))*COS(W4(I))*COS(W5(I))
Z26(I)=SIN(W1(I))*SIN(W2(I))*COS(W3(I))*COS(W4(I))*SIN(W5(I))
Z27(I)=SIN(W1(I))*SIN(W2(I))*COS(W3(I))*SIN(W4(I))*COS(W5(I))
Z28(I)=SIN(W1(I))*SIN(W2(I))*COS(W3(I))*SIN(W4(I))*SIN(W5(I))
Z29(I)=SIN(W1(I))*SIN(W2(I))*SIN(W3(I))*COS(W4(I))*COS(W5(I))
Z30(I)=SIN(W1(I))*SIN(W2(I))*SIN(W3(I))*COS(W4(I))*SIN(W5(I))
Z31(I)=SIN(W1(I))*SIN(W2(I))*SIN(W3(I))*SIN(W4(I))*COS(W5(I))
Z32(I)=SIN(W1(I))*SIN(W2(I))*SIN(W3(I))*SIN(W4(I))*SIN(W5(I))
NEXT I
FOR X=0 TO 6 STEP Fs
X1=360*X
Re2=0
Im2=0
Re3=0
Im3=0
Re4=0
Im4=0
Re5=0
Im5=0
Re6=0
Im6=0
Re7=0
Im7=0
Re8=0
Im8=0
Re9=0
Im9=0
Re10=0
```

```
Im10=0
Re11=0
Im11=0
Re12=0
Im12=0
Re13=0
Im13=0
Re14=0
Im14=0
Re15=0
Im15=0
Re16=0
Im16=0
Re17=0
Im17=0
Re18=0
Im18=0
Re19=0
Im19=0
Re20=0
Im20=0
Re21=0
Im21=0
Re22=0
Im22=0
Re23=0
Im23=0
Re24=0
Im24=0
Re25=0
Im25=0
Re26=0
Im26=0
Re27=0
Im27=0
Re28=0
Im28=0
Re29=0
Im29=0
Re30=0
Im30=0
Re31=0
Im31=0
Re32=0
Im32=0
FOR K=1 TO J-1
IF Z2(K)<>0 THEN Re2=Re2+Ts*Z2(K)*COS(X1*Tm1(K))
IF Z2(K)<>0 THEN Im2=Im2-Ts*Z2(K)*SIN(X1*Tm1(K))
IF Z3(K)<>0 THEN Re3=Re3+Ts*Z3(K)*COS(X1*Tm1(K))
IF Z3(K)<>0 THEN Im3=Im3-Ts*Z3(K)*SIN(X1*Tm1(K))
IF Z4(K)<>0 THEN Re4=Re4+Ts*Z4(K)*COS(X1*Tm1(K))
```

```
IF Z4(I) .NO THEN Im4=Im4-Ts*Z4(I)*SIN(X1*Tm1(I))
IF Z5(I) .O THEN Re5=Re5+Ts*Z5(I)*COS(X1*Tm1(I))
IF Z5(I) .NO THEN Im5=Im5-Ts*Z5(I)*SIN(X1*Tm1(I))
IF Z6(I) .O THEN Re6=Re6+Ts*Z6(I)*COS(X1*Tm1(I))
IF Z6(I) .NO THEN Im6=Im6-Ts*Z6(I)*SIN(X1*Tm1(I))
IF Z7(I) .O THEN Re7=Re7+Ts*Z7(I)*COS(X1*Tm1(I))
IF Z7(I) .O THEN Im7=Im7-Ts*Z7(I)*SIN(X1*Tm1(I))
IF Z8(I) .O THEN Re8=Re8+Ts*Z8(I)*COS(X1*Tm1(I))
IF Z8(I) .O THEN Im8=Im8-Ts*Z8(I)*SIN(X1*Tm1(I))
IF Z9(I) .O THEN Re9=Re9+Ts*Z9(I)*COS(X1*Tm1(I))
IF Z9(I) .O THEN Im9=Im9-Ts*Z9(I)*SIN(X1*Tm1(I))
IF Z10(I) .O THEN Re10=Re10+Ts*Z10(I)*COS(X1*Tm1(I))
IF Z10(I) .O THEN Im10=Im10-Ts*Z10(I)*SIN(X1*Tm1(I))
IF Z11(I) .O THEN Re11=Re11+Ts*Z11(I)*COS(X1*Tm1(I))
IF Z11(I) .O THEN Im11=Im11-Ts*Z11(I)*SIN(X1*Tm1(I))
IF Z12(I) .O THEN Re12=Re12+Ts*Z12(I)*COS(X1*Tm1(I))
IF Z12(I) .O THEN Im12=Im12-Ts*Z12(I)*SIN(X1*Tm1(I))
IF Z13(I) .O THEN Re13=Re13+Ts*Z13(I)*COS(X1*Tm1(I))
IF Z13(I) .O THEN Im13=Im13-Ts*Z13(I)*SIN(X1*Tm1(I))
IF Z14(I) .O THEN Re14=Re14+Ts*Z14(I)*COS(X1*Tm1(I))
IF Z14(I) .O THEN Im14=Im14-Ts*Z14(I)*SIN(X1*Tm1(I))
IF Z15(I) .O THEN Re15=Re15+Ts*Z15(I)*COS(X1*Tm1(I))
IF Z15(I) .O THEN Im15=Im15-Ts*Z15(I)*SIN(X1*Tm1(I))
IF Z16(I) .O THEN Re16=Re16+Ts*Z16(I)*COS(X1*Tm1(I))
IF Z16(I) .O THEN Im16=Im16-Ts*Z16(I)*SIN(X1*Tm1(I))
IF Z17(I) .O THEN Re17=Re17+Ts*Z17(I)*COS(X1*Tm1(I))
IF Z17(I) .O THEN Im17=Im17-Ts*Z17(I)*SIN(X1*Tm1(I))
IF Z18(I) .O THEN Re18=Re18+Ts*Z18(I)*COS(X1*Tm1(I))
IF Z18(I) .O THEN Im18=Im18-Ts*Z18(I)*SIN(X1*Tm1(I))
IF Z19(I) .O THEN Re19=Re19+Ts*Z19(I)*COS(X1*Tm1(I))
IF Z19(I) .O THEN Im19=Im19-Ts*Z19(I)*SIN(X1*Tm1(I))
IF Z20(I) .O THEN Re20=Re20+Ts*Z20(I)*COS(X1*Tm1(I))
IF Z20(I) .O THEN Im20=Im20-Ts*Z20(I)*SIN(X1*Tm1(I))
IF Z21(I) .O THEN Re21=Re21+Ts*Z21(I)*COS(X1*Tm1(I))
IF Z21(I) .O THEN Im21=Im21-Ts*Z21(I)*SIN(X1*Tm1(I))
IF Z22(I) .O THEN Re22=Re22+Ts*Z22(I)*COS(X1*Tm1(I))
IF Z22(I) .O THEN Im22=Im22-Ts*Z22(I)*SIN(X1*Tm1(I))
IF Z23(I) .O THEN Re23=Re23+Ts*Z23(I)*COS(X1*Tm1(I))
IF Z23(I) .O THEN Im23=Im23-Ts*Z23(I)*SIN(X1*Tm1(I))
IF Z24(I) .O THEN Re24=Re24+Ts*Z24(I)*COS(X1*Tm1(I))
IF Z24(I) .O THEN Im24=Im24-Ts*Z24(I)*SIN(X1*Tm1(I))
IF Z25(I) .O THEN Re25=Re25+Ts*Z25(I)*COS(X1*Tm1(I))
IF Z25(I) .O THEN Im25=Im25-Ts*Z25(I)*SIN(X1*Tm1(I))
IF Z26(I) .O THEN Re26=Re26+Ts*Z26(I)*COS(X1*Tm1(I))
IF Z26(I) .O THEN Im26=Im26-Ts*Z26(I)*SIN(X1*Tm1(I))
IF Z27(I) .O THEN Re27=Re27+Ts*Z27(I)*COS(X1*Tm1(I))
IF Z27(I) .O THEN Im27=Im27-Ts*Z27(I)*SIN(X1*Tm1(I))
IF Z28(I) .O THEN Re28=Re28+Ts*Z28(I)*COS(X1*Tm1(I))
IF Z28(I) .O THEN Im28=Im28-Ts*Z28(I)*SIN(X1*Tm1(I))
IF Z29(I) .O THEN Re29=Re29+Ts*Z29(I)*COS(X1*Tm1(I))
IF Z29(I) .O THEN Im29=Im29-Ts*Z29(I)*SIN(X1*Tm1(I))
```

```
IF Z30(I).0 THEN Re30=Re30+Ts*Z30(I.)*COS(X1*Tm1(I.))
IF Z30(I.) 0 THEN Im30=Im30-Ts*Z30(I.)*SIN(X1*Tm1(I.))
IF Z31(I.) 0 THEN Re31=Re31+Ts*Z31(I.)*COS(X1*Tm1(I.))
IF Z31(I.) 0 THEN Im31=Im31-Ts*Z31(I.)*SIN(X1*Tm1(I.))
IF Z32(I.) 0 THEN Re32=Re32+Ts*Z32(I.)*COS(X1*Tm1(I.))
IF Z32(I.) 0 THEN Im32=Im32-Ts*Z32(I.)*SIN(X1*Tm1(I.))
NEXT I
R1=Re2 2+Im2 2+Re3 2+Im3 2+Re4 2+Im4 2+Re5 2+Im5 2
R2=Re6 2+Im6 2+Re7 2+Im7 2+Re8 2+Im8 2+Re9 2+Im9 2
R3=Re10 2+Im10 2+Re11 2+Im11 2+Re12 2+Im12 2+Re13 2
R4=Im13 2+Re14 2+Im14 2+Re15 2+Im15 2+Re16 2+Im16 2
R5=Re17 2+Im17 2+Re18 2+Im18 2+Re19 2+Im19 2+Re20 2
R6=Im20 2+Re21 2+Im21 2+Re22 2+Im22 2+Re23 2+Im23 2
R7=Re24 2+Im24 2+Re25 2+Im25 2+Re26 2+Im26 2+Re27 2
R8=Im27 2+Re28 2+Im28 2+Re29 2+Im29 2+Re30 2+Im30 2
Rsb0=Re31 2+Im31 2+Re32 2+Im32 2+R1+R2+R3+R4+R5+R6+R7+R8
Rb11=Re2*Re3+Im2*Im3+Re3*Re5+Im3*Im5+Re4*Re7+Im4*Im7
Rb12=Re5*Re9+Im5*Im9+Re6*Re11+Im6*Im11+Re7*Re13+Im7*Im13
Rb13=Re8*Re15+Im8*Im15+Re9*Re17+Im9*Im17+Re10*Re19
Rb14=Im10*Im19+Re11*Re21+Im11*Im21+Re12*Re23+Im12*Im23
Rb15=Re13*Re25+Im13*Im25+Re27*Re14+Im14*Im27+Re15*Re29
Rsb1=Re16*Re31+Im16*Im31+Rb11+Rb12+Rb13+Rb14+Rb15
Ib11=Re3*Im2-Re2*Im3+Re5*Im3-Re3*Im5+Re7*Im4-Re4*Im7
Ib12=Re7*Im5-Re5*Im7+Re11*Im6-Re6*Im11+Re13*Im7-Re7*Im13
Ib13=Re15*Im8-Re8*Im15+Re17*Im9-Re9*Im17+Re19*Im10
Ib14=-Re10*Im19+Re21*Im11-Re11*Im21+Re23*Im12-Re12*Im23
Ib14=Re25*Im13-Re13*Im25+Re27*Im14-Re14*Im27+Re29*Im15
Isb1=-Re15*Im29+Re31*Im16-Re16*Im31+Ib11+Ib12+Ib13+Ib14
Rb21=Re2*Re5+Im2*Im5+Re3*Re9+Im3*Im9+Re4*Re13+Im4*Im13
Rb22=Re5*Re17+Im5*Im17+Re6*Re21+Im6*Im21+Re7*Re25
Rsb2=Im7*Im25+Re8*Re29+Im8*Im29+Rb21+Rb22
Ib21=Re5*Im2-Re2*Im5+Re9*Im3-Re3*Im9+Re13*Im4-Re4*Im13
Isb2=Re17*Im5-Re5*Im17+Re21*Im6-Re6*Im21+Re25*Im7
Isb2=Re25*Im7-Re7*Im25+Re29*Im8-Re8*Im29+Ib21
Rsb3=Re2*Re9+Im2*Im9+Re3*Re17+Im3*Im17+Re4*Re25+Im4*Im25
Isb3=Re9*Im2-Re2*Im9+Re17*Im3-Re3*Im17+Re25*Im4-Re4*Im25
Rsb4=Re2*Re17+Im2*Im17
Isb4=Re17*Im2-Re2*Im17
Ys1=Rsb0+2*(Rsb1*COS(X1)+Isb1*SIN(X1)+Rsb2*COS(2*X1))
Ys2=2*(Isb2*SIN(2*X1)+Rsb3*COS(3*X1)+Isb3*SIN(3*X1))
Y=2*(Rsb4*COS(4*X1)+Isb4*SIN(4*X1))+Ys1+Ys2
IF X=0 THEN Y2=Y
IF Y2  0 THEN Y=Y/Y2
IF Y =10 (-7) THEN Y=10 (-7)
M=M+1
Funct(M)=LGT(Y)
IF R=0 THEN
F0(M)=Funct(M)
ELSE
IF R=.5 THEN
F1(M)=Funct(M)
```

```
ELSE
F2(M)=Funct(M)
END IF
END IF
Xs(M)=X
PRINT Xs(M),Funct(M),Y,R
NEXT X
NEXT R
! ##################################################
!                  Graphic of PSD
! ##################################################
IF Vx<>0 THEN Rep
GINIT
GRAPHICS ON
INPUT "INPUT (S FOR SCREEN),(P FOR PLOTTER)",D$
IF D$="P" THEN
    PLOTTER IS 705,"HPGL"
ELSE
    PLOTTER IS 3,"INTERNAL"
END IF
VIEWPORT 25,110,35,85
WINDOW 0,7,0,6
AXES .1,.1,0,0,10,10,3
AXES .1,.1,7,6,10,10,3
CLIP OFF
CSIZE 2.5
LORG 6
MOVE 3.5,6.8
LABEL "Power Spectral Density (dB)"
LDIR -90
MOVE -.4,3
LABEL "x=fTb"
MOVE -.8,3
LABEL "Fig. 3.11 - Shaping function of duration 5Tb"
MOVE -1.2,3
LABEL "Sqrt raised cosine pulse"
LORG 8
FOR I=0 TO 7
MOVE I,6.1
LABEL USING "#,K";10*(I-7)
NEXT I
LORG 6
FOR I=0 TO 6
MOVE -.1,I
LABEL USING "#,K";6-I
NEXT I
P:      !
CLIP ON
CSIZE 2.3
FOR R=0 TO 1 STEP .5
IF R=0 THEN
```

```
LINE TYPE 1
Space=Space+.3
MOVE 6.6-Space,.6
LABEL "Alpha=";R
MOVE 6.5-Space,2
DRAW 6.5-Space,1.2
MOVE 7,6
FOR I=1 TO M
DRAW 7+F0(I),6-Xs(I)
NEXT I
PENUP
ELSE
IF R=.5 THEN
Space=Space+.3
MOVE 6.6-Space,.6
LABEL "Alpha=";R
LINE TYPE 6
MOVE 6.5-Space,2
DRAW 6.5-Space,1.25
MOVE 7,6
FOR I=1 TO M
DRAW 7+F1(I),6-Xs(I)
NEXT I
PENUP
ELSE
Space=Space+.3
LINE TYPE 1
MOVE 6.6-Space,.6
LABEL "Alpha=";R
LINE TYPE 8
MOVE 6.5-Space,2
DRAW 6.5-Space,1.2
MOVE 7,6
FOR I=1 TO M
DRAW 7+F2(I),6-Xs(I)
NEXT I
PENUP
END IF
END IF
BEEP
Vx=Vx+1
NEXT R
GOTO New_curve
STOP
END
```

APPENDIX D

BER COMPUTATION

The program to compute the probability of error at the receiver is given below

```
!            BER Computation
!       before and after the LPF
! ***************************************************
V%=0
DEG
alpha:
INPUT "WHAT IS THE LINE TYPE",L
LINE TYPE L
INPUT "WHAT IS THE VALUE OF ACCURACY N",N
INPUT "WHAT IS THE VALUE OF ALPHA",R
Ts=180/N
Wmax=2*N
DIM Fs(2000),X%(2000),Ht(2000),Fy(2000),Fy0(2000)
DIM Fs1(2000),Qc(2000),Phie(2000),P0(2000),P1(2000)
DIM P4(2000),Fy3(2000),Fy4(2000),Pe3(100),Xe3(100)
DIM Fy1(2000),Fy2(2000),P2(2000),P3(2000)
Ts2=1.E-7
Ts1=1
T12=Ts2
E=-1
FOR T1=0 TO T12 STEP Ts2
E=E+1
Ht(E)=.5/T12
PRINT E,Ht(E)
NEXT T1
Z1=-1
FOR Db=0 TO 10 STEP Ts1
Snr=10^(Db/10)
PRINT Snr
M=-1
FOR I=-N TO N-1
'*****************************************
!          Error function: erf(x)
'*****************************************
Fct=1
```

```
X5=COS(1*Ts)
Xn=SQR(Snr)*X5
Erf=2*Xn/SQR(PI)
FOR S=1 TO 150
Fct=Fct*S
Ct2=Fct*(2*S+1)
W0=2*(-1)^S*Xn^(2*S+1)/(Ct2*SQR(PI))
IF ABS(W0)<1.E-300 THEN Srt
Erf=Erf+W0
NEXT S
:
'*****************************************
! p.d.f of the phase at the input of the filter.
'*****************************************
M=M+1
Fs(M)=EXP(-Snr)*(1+SQR(Snr*PI)*X5*EXP(Snr*X5^2)*(1+Erf))/(2*PI)
PRINT Fs(M)
NEXT I
'#########################################################
!   Calculation of the caracteristic function.
!#########################################################
FOR I2=0 TO E
'IF ABS(Ht(I2))<1.E-15 THEN Cn
FOR U=0 TO N-1
X2=U*Ht(I2)*Ts^2
Oc(U)=0
FOR I=0 TO M
Oc(U)=Oc(U)+Fs(I)*COS((-N+I)*X2*Ts)*PI/N
NEXT I
Oc(U)=Oc(U)^2
PRINT Oc(U),U,I2
NEXT U
IF I2=0 THEN
FOR I=0 TO N-1
Phie(I)=Oc(I)
NEXT I
ELSE
FOR I=0 TO N-1
Phie(I)=Phie(I)*Oc(I)^2
NEXT I
END IF
:
NEXT I2
'#########################################
!     Calculation of the p.d.f.
'#########################################
Ar2=0
FOR I=0 TO N-1
Fy(I)=.5*Phie(0)/PI
FOR J=1 TO N-1
Fy(I)=Fy(I)+Phie(J)*COS(J*I*Ts)/PI
```

```
NEXT J
Xs(I)=4*I/N
IF Xs(I)>=2 THEN Ar2=Ar2+Fy(I)*PI/N
PRINT Fy(I),Xs(I),Ar2
NEXT I
Z1=Z1+1
Pe3(Z1)=2*Ar2
Xe3(Z1)=Db
'*****************************************
IF Db=0 THEN
FOR I=0 TO N-1
Fy0(I)=Fy(I)
NEXT I
FOR I=0 TO N-1
P0(I)=Phase(I)
NEXT I
ELSE
IF Db=0.1 THEN
FOR I=0 TO N-1
Fy1(I)=Fy(I)
NEXT I
FOR I=0 TO N-1
P1(I)=Phase(I)
NEXT I
ELSE
IF Db=0.2 THEN
FOR I=0 TO N-1
Fy2(I)=Fy(I)
NEXT I
FOR I=0 TO N-1
P2(I)=Phase(I)
NEXT I
ELSE
FOR I=0 TO N-1
Fy3(I)=Fy(I)
NEXT I
FOR I=0 TO N-1
P3(I)=Phase(I)
NEXT I
END IF
END IF
END IF
NEXT Db
FOR I=0 TO Z1
PRINT Pe3(I)
NEXT I
!#################################################
'     Plot of the caracteristic function.
'#################################################
INPUT "PDF (D),Characteristic funct(C)",Hj$
IF Hj$="D" THEN Pdf
```

```
GINIT
INPUT "WRITE (S FOR SCREEN),(P FOR PLOTTER )",D$
IF D$="P" THEN
PLOTTER IS 705,"HPGL"
ELSE
PLOTTER IS 3,"INTERNAL"
END IF
GRAPHICS ON
VIEWPORT 15,120,15,90
FRAME
WINDOW 0,40,0,2
AXES 5,.1,0,0,10,5,3
CLIP OFF
CSIZE 3
LORG 6
FOR I=0 TO 40 STEP 5
MOVE I,-.05
LABEL I
NEXT I
LORG 8
FOR I=.5 TO 1.5 STEP .5
MOVE -.0005,I
LABEL I
NEXT I
MOVE 35,-.7
LABEL "Characteristic Function of the RV after the Filter"
CLIP ON
CSIZE 2.3
PENUP
FOR Db=0 TO 10 STEP Ts1
IF Db=1 THEN
MOVE 39.5,1.7
LABEL "SNR=";Db;"dB"
MOVE 30,1.7
DRAW 34,1.7
PENUP
PLOT 0,P0(0)
FOR I=0 TO N-1
DRAW I,P0(I)
NEXT I
PENUP
ELSE
IF Db=0+Ts1 THEN
Space=Space+.1
MOVE 39.5,1.7-Space
LABEL "SNR=";Db;"dB"
LINE TYPE 5
MOVE 30,1.7-Space
DRAW 34,1.7-Space
PENUP
PLOT 0,P1(0)
```

```
FOR I=0 TO N-1
DRAW I,P1(I)
NEXT I
PENUP
ELSE
IF Db=0.2*Ts1 THEN
Space=Space+.1
LINE TYPE 1
MOVE 29.5,1.7-Space
LABEL "SNR=";Db;"dB"
LINE TYPE 6
MOVE 30,1.7-Space
DRAW 34,1.7-Space
PENUP
PLOT 0,P2(0)
FOR I=0 TO N-1
DRAW I,P2(I)
NEXT I
PENUP
ELSE
Space=Space+.1
LINE TYPE 1
MOVE 29.5,1.7-Space
LABEL "SNR=";Db;"dB"
LINE TYPE 7
MOVE 30,1.7-Space
DRAW 34,1.7-Space
PENUP
PLOT 0,P3(0)
FOR I=0 TO N-1
DRAW I,P3(I)
NEXT I
PENUP
END IF
END IF
END IF
NEXT Db
PENUP
!
!*************************************
!    plot of the power density function
!*************************************
Space=0
GINIT
INPUT "S FOR SCREEN,P FOR PLOTTER",L$
IF L$="P" THEN
PLOTTER IS 705,"HPGL"
ELSE
PLOTTER IS 3,"INTERNAL"
END IF
GRAPHICS ON
```

```
VIEWPORT 10,120,10,90
FRAME
WINDOW 0,4,0,5
AXES .1,.1,0,0,10,10,3
AXES .1,.1,4,5,10,10,3
CLIP OFF
CSIZE 2.3
LORG 6
FOR I=0 TO 4
MOVE I,-.01
LABEL 45*I
NEXT I
LORG 8
FOR I=0 TO 5
MOVE -.05,I
LABEL I
NEXT I
MOVE 2.8,-.5
LABEL "p.d.f of the RV after the filter"
FOR Db=0 TO 10 STEP Ts1
IF Db=0 THEN
LINE TYPE 1
MOVE 3.98,4.5
LABEL "SNR=";Db;"dB"
MOVE 3.98,4.4
LABEL "Alpha=";R
MOVE 3.1,4.5
DRAW 3.4,4.5
PENUP
PLOT 0,Fy0(0)
FOR I=0 TO N-1
DRAW Xs(I),Fy0(I)
NEXT I
PENUP
ELSE
IF Db=0+Ts1 THEN
Space=Space+.3
LINE TYPE 1
MOVE 3.98,4.5-Space
LABEL "SNR=";Db;"dB"
MOVE 3.98,4.4-Space
LABEL "Alpha=";R
PENUP
LINE TYPE 5
MOVE 3.1,4.5-Space
DRAW 3.4,4.5-Space
PENUP
PLOT 0,Fy1(0)
FOR I=0 TO N-1
DRAW Xs(I),Fy1(I)
NEXT I
```

```
PENUP
ELSE
IF Db=0+2*Ts1 THEN
Space=Space+.3
LINE TYPE 1
MOVE 3.95,4.5-Space
LABEL "SNR=";Db;"dB"
MOVE 3.98,4.4-Space
LABEL "Alpha=";R
PENUP
LINE TYPE 6
MOVE 3.1,4.5-Space
DRAW 3.4,4.5-Space
PENUP
PLOT 0,Fy2(0)
FOR I=0 TO N-1
DRAW Xs(I),Fy2(I)
NEXT I
PENUP
ELSE
Space=Space+.3
LINE TYPE 1
MOVE 3.95,4.5-Space
LABEL "SNR=";Db;"dB"
MOVE 3.98,4.4-Space
LABEL "Alpha=";R
PENUP
LINE TYPE 7
MOVE 3.1,4.5-Space
DRAW 3.4,4.5-Space
PENUP
PLOT 0,Fy3(0)
FOR I=0 TO N-1
DRAW Xs(I),Fy3(I)
NEXT I
PENUP
END IF
END IF
END IF
NEXT Db
form:
Space=0
GINIT
INPUT "(S FOR SCREEN),(P FOR PLOTTER)",D$
IF D$="P" THEN
PLOTTER IS 705,"HPGL"
ELSE
PLOTTER IS 3,"INTERNAL"
END IF
GRAPHICS ON
VIEWPORT 15,120,10,90
```

```
WINDOW 0,9,0,10
FRAME
CLIP OFF
Dy=.1
LORG 8
FOR Decade=0 TO 9
FOR Unit=1 TO 1+8*(Decade<9)
Y=Decade+LGT(Unit)
MOVE Y,10
DRAW Y,9.9
IF Y=Decade THEN DRAW Y,9.8
NEXT Unit
NEXT Decade
LDIR -90
FOR Y=0 TO 8 STEP Dy*10
LORG 8
CSIZE 3
MOVE Y,10.1
LABEL USING "#,K";"10"
CSIZE 2
LORG 1
MOVE Y+.1,10.30
LABEL USING "#,K";Y-9
NEXT Y
LORG 8
CSIZE 3
MOVE 9,9.9
LABEL 1
LORG 6
FOR I=0 TO 10
MOVE 0,I
DRAW .1,I
MOVE -.1,I
LABEL 10-I
NEXT I
MOVE -.5,5
LABEL "Signal to Noise ratio (dB)"
LDIR 0
MOVE 4.5,11.0
LABEL "Probability of error"
PENUP
MOVE 9,10
FOR I=0 TO 10 STEP .1
DRAW LGT(.5*EXP(-10^(I/10)))+9,10-I
PRINT LGT(.5*EXP(-10^(I/10))),I
NEXT I
MOVE 9+LGT(Pe3(0)),10-Xe3(0)
FOR I=0 TO Z1
DRAW 9+LGT(Pe3(I)),10-Xe3(I)
NEXT I
PENUP
STOP
END
```